

**Applications of Water Stable Metal-Organic Frameworks**

Journal:	<i>Chemical Society Reviews</i>
Manuscript ID	CS-REV-05-2016-000362.R1
Article Type:	Review Article
Date Submitted by the Author:	21-Jun-2016
Complete List of Authors:	Wang, Chenghong; Imperial College London, Chemical Engineering; National University of Singapore, 28 Medical Drive, 117456, Singapore, NUS Graduate School for Integrative Sciences & Engineering ; National University of Singapore, 10 Kent Ridge, 117576, Singapore, Department of Civil and Environmental Engineering Liu, Xinlei; Imperial College London, Chemical Engineering Keser Demir,, Nilay; Imperial College London, Chemical Engineering Chen, J. Paul; National Univ of Singapore, Li, Kang; Imperial College London, Chemical Engineering



Journal Name

ARTICLE

Applications of Water Stable Metal-Organic Frameworks

Chenghong Wang,^{abc} Xinlei Liu,^a Nilay Keser Demir,^a J. Paul Chen,^{bc} and Kang Li^{a*}

Received 00th January 20xx,
Accepted 00th January 20xx

DOI: 10.1039/x0xx00000x

www.rsc.org/

The recent advancement of water stable metal-organic frameworks (MOFs) expands the application of this unique porous material. This review article aims at studying their applications in terms of five major areas: adsorption, membrane separation, sensing, catalysis, and proton conduction. These applications are either conducted in a water-containing environment or directly targeted on water treatment processes. The representative and significant studies in each area were comprehensively reviewed and discussed for perspectives, to serve as a reference for researchers working in the related areas. At the end, a summary and future outlook on the applications of water stable MOFs are suggested as concluding remarks.

1. Introduction

Water stability is a crucial property for any materials to be industrially applicable since water is abundant in the preparation, storage, transportation and application processes. Metal-organic frameworks (MOFs), a new type of porous materials, have attracted substantial attention in the last decade. They are typically comprised of inorganic metal ions or metal clusters linked by organic ligands through coordination bonds.^{1,2} The formed porous structures with pores of molecular dimensions are associated with a series of desirable properties such as low density, high surface area and high porosity.³ Scientists believe that MOFs are preferred over the conventional porous materials such as zeolites and carbon-based materials in certain areas, owing to their customizable chemical functionalities, versatile architectures and milder synthesis conditions.⁴⁻⁸ This is because, in essence, MOFs can be assembled from plenty of building blocks, which accommodates an infinite number of special structures and potential applications. Moreover, the mild synthesis conditions of MOFs allow for the introduction of a variety of delicate functionalities into the framework. As a result of all these advantages, MOFs have been proposed by researchers for a range of applications including gas storage, separation, sensing, catalysis, proton conduction, etc.^{1,2} However, due to the lability of ligand-metal bonds, most of the earlier reported MOFs are sensitive to water content.^{9,10} For instance, one of

the milestone MOFs, MOF-5,¹¹ decomposes gradually when the environment contains moisture.¹² The instability in water has considerably limited these MOFs' further application and commercialisation, since water or moisture is usually present in most industrial processes as mentioned. Hence, water stable MOFs have been on great demand in the scientific community.

Water stable MOFs by definition are classified as those that do not exhibit structural breakdown under exposure to water content. In principle, the key criterion to determine if a MOF structure stays stable in the water stability test is through the comparison of the typical chemical characteristics between post-exposure samples and pristine samples. The chemical characteristics can be the powder X-ray diffraction (PXRD) pattern and BET surface area on the basis of gas adsorption capacity, which could well suggest whether the MOF loses its crystallinity or structural porosity after the exposure to water content. Generally, MOF structures are susceptible to the attack by water molecules, which would lead to ligands displacement, phase changes, and structural decomposition. A water stable MOF structure must be strong enough to prevent the intrusion of water molecules into the framework, and the consequent losses in crystallinity and overall porosity. Thus, MOF structures with a great stability normally possess strong coordination bonds (thermodynamic stability) or significant steric hindrance (kinetic stability), to prevent the detrimental hydrolysis reaction which breaks the metal-ligand bonds.¹³ With the improved understanding towards MOF structural stability in water system and constant efforts, a number of research publications on water stable MOF are now experiencing a surge, and plenty more water stable MOFs are reported every year. Thus far, a consolidated database of water stable MOFs has been established owing to the significant work by Burtch *et al.*,¹³ Canivet *et al.*,¹⁴ Howarth *et al.*,¹⁵ etc. Basically, water stable MOFs could be categorised into three major types: (1) metal carboxylate frameworks consisting of high-valence metal ions; (2) metal azolate frameworks containing nitrogen-donor ligands; (3) MOFs

^a Department of Chemical Engineering, Imperial College London, London SW7 2AZ, United Kingdom. Corresponding author, Email: kang.li@imperial.ac.uk

^b NUS Graduate School for Integrative Sciences and Engineering, National University of Singapore, Singapore 117456, Singapore.

^c Department of Civil and Environmental Engineering, National University of Singapore, Singapore 119260, Singapore.

† Footnotes relating to the title and/or authors should appear here.

Electronic Supplementary Information (ESI) available: [details of any supplementary information available should be included here]. See DOI: 10.1039/x0xx00000x

functionalized by hydrophobic pore surfaces or with blocked metal ions.¹⁶

When all the coordination environments remain the same, high-valence metal ions with high charge density could form a stronger coordination bond towards the ligands. This trend has been widely observed by MOF material researchers, and rationalised by the hard/soft acid-base principle.¹⁶ On the other hand, high-valence metal units with higher coordination number normally result in a greatly rigid structure, making the metal sites less susceptible to water molecules.¹⁷ Thus, with the most commonly used carboxylate-type ligands, high-valence metal ions, such as Fe³⁺, Cr³⁺, and Zr⁴⁺, have been exploited to synthesise water stable MOFs. For instance, Ferey and his co-workers developed the famous Fe-based MIL-100 and Cr-based MIL-101, which could provide decent chemical stability, staying robust for months in ambient environment and various solvents.¹⁸ In addition, MOFs containing high-valence Zr⁴⁺ cations, like the well-known UiO-66 and PCN family, demonstrate remarkable hydro-stability even at the acidic and some basic conditions.^{19, 20} Following this path, a range of water stable MOFs have been synthesised and reported in recent years, for example: (1) Zr-based PCN-228/-229/-230,²¹ PCN-521,²² PCN-777,²³ NU-1000,²⁴ NU-1105,²⁵ MOF-808,²⁶ MIL-160,²⁷ MIL-163,²⁸ FJI-H6,²⁹ [Zr₆O₄(OH)₄(btba)₃](DMF)_x(H₂O)_y,³⁰ (2) Hf-based PCN-523,²² FJI-H7,²⁹ (3) lanthanide element-based [La(py₂dc)_{1.5}(H₂O)₂]_n·2H₂O,³¹ [(Dy(Cmdcp)(H₂O)₃](NO₃)₂·2H₂O)_n,³² [Eu(HL)(H₂O)₂]_n·2H₂O,³³ Tb-DSOA,³⁴ [Tb(L)(OH)]_x(sol_v)_y,³⁵ ([Tb(L₁)_{1.5}(H₂O)]_n·3H₂O)_n,³⁶ (4) In-based JLU-Liu18,³⁷ InPCF-1;³⁸ (5) Al-based MIL-121,³⁹ CAU-10,⁴⁰ etc.

Besides the utilization of high-valence metals as hard acids for constructing water stable MOFs, exploiting the azolate ligands (such as imidazolates, pyrazolates, triazolates, tetrazolates, etc.) is another strategy in water stable MOF synthesis.⁴¹ As these nitrogen-containing ligands are generally softer ligands, when they interact with the softer divalent metal ions, stronger MOF structures can be formed as a result. The most representative example of this category is the zeolitic imidazolate frameworks (ZIFs), using Zn²⁺/Co²⁺ together with imidazolate linkers to construct a variety of stable crystals analogous to zeolite topology.⁴²⁻⁴⁴ Also, Colombo *et al.* developed the microporous pyrazolate-based MOFs, M₃(BTP)₂ (M = Ni, Cu, Zn, Co), which exhibited a great hydrothermal stability compared to most carboxylate-based MOFs.⁴⁵ Following this strategy, there are more and more azolate-based MOFs exhibiting fair level of hydro-stability developed in recent years, including: MAF series materials (e.g. MAF-6, MAF-7, MAF-49, MAF-X8, etc.) developed by Chen's group;⁴⁶⁻⁵⁰ and also FIR-54,⁵¹ [Zn₁₂(trz)₂₀][SiW₁₂O₄₀]_n·11H₂O,⁵² [Zn(trz)(H₂betc)_{0.5}]_n·DMF,⁵³ Zn₂TCS(4,4'-bipy),⁵⁴ Zn-pbdc-11a(bpe)/-12a(bpe)/-12a(bpy),⁵⁵ Zn(IM)_{1.5}(abIM)_{0.5},⁵⁶ ([Zn(C₁₀H₂O₈)_{0.5}(C₁₀S₂N₂H₈)_n·5H₂O)_n,⁵⁷ Co/Zn-BTTBPPY,⁵⁸ [Co₄L₃(μ₃-OH)(H₂O)₃](SO₄)_{0.5},⁵⁹ Cu₂L,⁶⁰ Cu₆(trz)₁₀(H₂O)₄[H₂SiW₁₂O₄₀]_n·8H₂O,⁶¹ [Ni(BPEB)],⁶² PCN-601,⁶³ [Eu₃(bpydb)₃(HCOO)(μ₃-OH)₂(DMF)]_n·(DMF)₃(H₂O)₂,⁶⁴ Mg-CUK-1,⁶⁵ [Cd₂(TBA)₂(bipy)(DMA)₂]_n,⁶⁶ etc.

In addition to increase metal-ligand bond strength, MOFs could be specifically functionalised for steric hindrance to sustain the robustness in an aqueous medium. Through introducing hydrophobic pore surfaces or blocked metal ions, water molecules can be excluded from approaching the lattice and attacking the framework structure. Plenty of case studies have been reported for the enhanced hydrothermal stability of MOFs: (1) Taylor *et al.* showed that nonpolar alkyl functional groups in CALF-25 allow the structure to adsorb appreciable amounts of water but remain structurally stable due to functional group shielding around the metal centre.⁶⁷ (2) Omary and his co-workers developed a series of fluorinated MOFs (FMOFs), which are superhydrophobic and exhibit remarkable water stability.^{68, 69} (3) Post synthetic approaches (e.g. ligand modification,⁷⁰ metal⁷¹ and ligand exchange reactions⁷²) were developed to considerably enhance the hydrophobicity and hydrothermal stability of the MOF structures that were already available.

On top of these three main types of water stable MOFs, the unceasing efforts to develop more and more water stable MOFs expand the applications of this unique class of porous material. With the advantage of being stable in water-involved environment, water stable MOFs can be effectively applied in a wide range of areas. Classical examples include applying the water stable MOFs for adsorption in both gaseous and liquid phases,⁷³⁻⁷⁵ for proton conduction with the aid of water,^{14, 76-79} as well as for sensing and catalysis when water content is present;⁸⁰⁻⁸⁴ besides, assembling the water stable MOF materials to thin films or membranes has a promising potential to further improve the effectiveness and efficiency of many industrial processes like water involved separation and waste water decontamination.⁸⁵ Promising performance has been observed owing to the undeniable advantages of MOF-type materials, such as huge porosity, easy tunability of their pore size, and multiple shapes from micro- to meso-porous scale through modifying the connectivity of inorganic moieties and the nature of organic linkers.

Herein, we systematically reviewed the applications of water stable MOFs in five major areas: adsorption, membrane separation, sensing, catalysis, and proton conduction. Meaningful studies in each of these five fields, where water content is present or directly involved, were comprehensively discussed. Taken together, this review could work as a useful reference with respect to water stable MOFs and their water-related applications. It would provide significant insights on MOF research and could lead to more advanced functional materials in respective industries.

(Note 1: for the ease of reading and picking up critical information, every **water stable MOF** and its **particular applications** are highlighted in bold at the discussion below.)

(Note 2: full names, the molecular structural information as well as the ligand abbreviations with respect to all the MOFs mentioned in this review is provided at the end, *Appendix*.)

2. Adsorption

Adsorption is one of the most effective processes to uptake specific compounds from liquid or gas phases. It is generally preferred because of the ease in operation, great efficiency and cost effectiveness. It has been widely studied not only in theoretical research but also for industrial development. To achieve desirable adsorption performance, it is always important to understand and design the proper process, and also to develop the functional adsorbent materials for relevant applications.

Currently, most commercially used adsorbents include activated carbon, mesoporous silica, zeolite, etc.^{86,87} As a class of recently developed porous materials, MOFs have shown huge potential in adsorption-related applications.⁸⁸ The unique structural characteristics, facile functionalization and tunable porosities render MOFs to be superior over other conventional porous materials.¹⁴ Besides, as a hybrid of inorganic and organic materials, MOFs is associated with a milder synthesis condition. With a great availability of various configuration and structures, as well as higher porosity and surface area, MOF is expecting to be a high-capacity adsorbent. Surveying the current literature, researchers have managed to employ water stable MOFs in both water adsorption/dehumidification and adsorptive removal of various targeted compounds in the presence of water. Generally, they provided a better performance in comparison with the conventional porous materials. On the basis of these studies, it was suggested that water stable MOFs could work as promising adsorbents in the field of liquid or gas phase adsorptions, which allows for a widespread applicability of MOF materials.

2.1 Water adsorption

Water adsorption properties are directly related with the applicability of the MOF. Comprehensive studies on the fundamental and practical aspects of water adsorption in MOFs have been conducted by Kungsgens *et al.*,⁸⁹ Canivet *et al.*,¹⁴ etc. Herein, to avoid repetition, we would not discuss the water adsorption performance of those MOFs that have been considered by them. In the work by Canivet and his co-workers, a representative set of MOFs was systematically examined and the typical mechanisms of water adsorption by MOFs were suggested to be: reversible and continuous pore filling, irreversible and discontinuous pore filling through capillary condensation, and irreversibility arising from the flexibility and possible structural modifications of the host material. Based on their summary, it can be found that most favourable MOFs for water adsorption and stability are the MIL-materials, i.e., **MIL-101** and **MIL-100**, which are the typical hydrophilic mesoporous compounds. They can capture water at very low relative pressure with a steep uptake behaviour, majorly owing to their specific structural features, i.e. topologically large pore size and volume, great BET surface area, as well as hydrophilic functional groups as adsorption sites. Moreover, compared to the typical silica gel, zeolites and porous carbon, MOF materials could provide a competitive or even superior performance. Owing to the fact that MOFs

exhibit a great diversity in terms of pore size, pore structure, inorganic clusters, and chemical functionality, MOF materials can provide various water uptake profiles to meet different application purposes.

Further to that, water adsorption in porous materials is important for many applications requiring capture and release of water such as dehumidification, thermal batteries, and delivery of drinking water in remote areas. In order to be viable in such water capture applications, Furukawa *et al.*⁹⁰ identified three criteria: first, low relative pressure pore filling or condensation of water into the pores of solid that exhibits steep uptake behaviour; second, high water uptake capacity for maximum delivery of water and facile adsorption/desorption processes for energy efficiency; third, high cycling performance and water stability. They examined a series of typical zirconium-based MOFs for water adsorption as shown in Fig. 1. It was found that two specific members, **MOF-801** and **MOF-841**, could swiftly capture water at well-defined, low relative pressure values and exhibit high uptake, recyclability, and water stability. The test results suggest that structural factors, like the cavity and pore size, prompt the formation of hydrogen bond between the water stable MOFs and neighbouring water molecules. Based on that, we can see the importance of intermolecular interaction between adsorbed water molecules within the water sorbents.

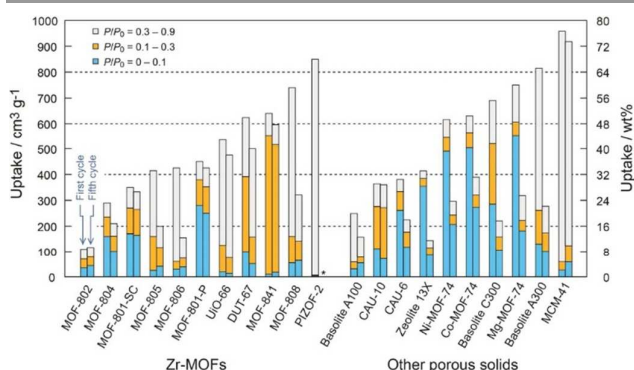


Figure 1. Water uptake capacity of zirconium MOFs (LHS) and other representative porous materials (RHS) in different pressure ranges. Left and right bars represent first and fifth adsorption cycles, respectively.⁹⁰ Reproduced from Ref. 90 with permission, copyright American Chemical Society, 2014.

Besides, Cadiou *et al.* developed the hydrothermally stable **MIL-160** as a hydrophilic water adsorbent.²⁷ Through strategic designs, the MOF adsorbent exhibits a very high uptake in the water sorption experiments, especially exceeding that of commercial benchmark porous solid SAPO-34. Taken into consideration of its excellent hydro-thermal stability, the MOF adsorbent is an ideal candidate for heat transfer applications. Also, Begum *et al.* introduced a new microporous cobalt triazolyl phosphonate MOF, $[\text{Co}_4\text{L}_3(\mu_3\text{-OH})(\text{H}_2\text{O})_3](\text{SO}_4)_{0.5}\cdot x\text{H}_2\text{O}$, which also exhibits exciting features for water adsorption.⁵⁹ This MOF possesses great water stability, and provides reversible hydration–dehydration behaviour with steep water uptake at low water vapour pressures. Moreover, Plessius *et al.*³¹ reported a new lanthanide MOF, built from lanthanum

ARTICLE

Journal Name

and pyzdc ligand. This MOF, $[\text{La}(\text{pyzdc})_{1.5}(\text{H}_2\text{O})_2] \cdot 2\text{H}_2\text{O}$, has a stable microporous structure with hydrophilic 1D tetragonal channels, and its window size is appropriate for accommodating water molecules. It was found that this framework is highly robust to dehydration/hydration cycles, since the large coordination spheres and flexible coordination geometries of lanthanide ions can facilitate structural re-organization without disrupting the overall framework. And also it is even thermally stable at high temperatures. This is one typical lanthanide MOF showing highly selective water adsorption, which opens exciting opportunities for removing water content from water/alcohol mixtures or wet gases.

2.2 Adsorption of targeted compounds

In addition to pure water adsorption, MOF based adsorbents have also shown promising results in capturing specific compounds from water environments (Tab. 1).^{73, 91} Water stable MOFs could be applied to effectively uptake gases in moisture conditions; also increasing number of research has been conducted to explore the viability of using water stable MOFs for wastewater remediation and efficient recovery of specific chemical components from water system. Targeted compounds existing in water systems include: SO_x, NO_x, greenhouse gases, VOCs; dyes, drugs and pharmaceuticals, organic chemicals, metal ions, etc.

Compared with the conventional adsorbents, MOFs are associated with higher accessible surface area and more active sites for the adsorption taking place. Its crystalline structure with well-defined space and passage channels leads to a new strategy that conquers the dilemma between the excellent properties from nanoscale effect and the aggregation of small size particles in the adsorption application of nanoparticle materials.⁹² Nevertheless, to be suitable in the targeted applications, MOFs as porous coordination materials must possess great chemical stabilities under different harsh conditions. With the sufficient chemical stability, it is anticipated that water stable MOFs could be one of the most powerful adsorbent materials contributing to an energy efficient and cost effective separation process.

Table 1. Adsorption of targeted compounds using water stable MOFs

Water stable MOF	Target compounds	Water extent	Capacity	Ref.
Co-MOF-74	Ammonia	80% RH	4.30 mol/kg	93
$[\text{Zn}_4(\mu_4\text{-O})-(\mu_4\text{-4-carboxy-3,5-dimethyl-4-carboxy-pyrazolato})_3]$	VOCs (Sarin & mustard gas)	Ambient moisture	$1.8 \text{ m}^3/\text{m}^3$	94
PCP-33	C ₂ H ₂	Ambient moisture	121.8 cm ³ /g	95
NU-1100	H ₂ & CH ₄	Ambient moisture	0.092 g/g & 0.27 g/g	96
IRMOF-74-III-CH ₂ NH ₂	CO ₂	65% RH	3.2 mmol/g	97

	Zn-pbdc-12a(bpe)	CO ₂	After exposure to water vapour	98 cm ³ /g	55
	mnen-Mg ₂ (dobpdc)	CO ₂	After exposure to water	3.5 mmol/g	98
	MAF-X25ox	CO ₂	82% RH	7.1 mmol/g	99
	FMOF-1	C ₆ -C ₈ hydrocarbons of oil components	100% RH	200~300 kg/m ³	69
	MAF-6	Methanol, ethanol, benzene, etc.	Water wet	-	50
Organic adsorption	UiO-66-NH ₂ @MON	Toluene	Water solution	0.15 ± 0.04 mL	100
	ZIF-8	Hydroxymethylfurfural	Water solution	465 mg/g	101
	CAU-1	Nitrobenzene	Water solution	970 mg/g	102
	ZIF-67	Benzotriazole	Water solution	163 mg/g	103
	MIL-68	Phenol	Water solution	341.1 mg/g	104
	MIL-101	Uranine	Water solution	127 mg/g	105
	$[(\text{C}_2\text{H}_5)_2\text{NH}_2]_2[\text{Mn}_6(\text{L})(\text{OH})_2(\text{H}_2\text{O})_6] \cdot 4\text{DEF}$	Methyl blue	Water solution	-	75
	UiO-67	Glyphosate and glufosinate	Water solution	537 mg/g	106
	UiO-66	Methylchlorophenoxypropionic acid	Water solution	370 mg/g	107
	ZIF-8	Phthalic acid	Water solution	654 mg/g	108
Ions adsorption	UiO-68-P(O)(OEt) ₂	Uranium	Water solution	217 mg/g	109
	NU-1000	Selenium and sulphate	Water solution	95, 56 mg/g	110 111
	FIR-54	Dichromate	Water solution	103 mg/g	51
	UiO-66	Arsenic	Water solution	303 mg/g	112
	MIL-96	Fluoride	Water solution	31.7 mg/g	113

2.2.1 Gases

Gaseous components including nitrogen-/sulphur-containing compounds, volatile organic compounds (VOCs) and greenhouse gases are normally mixed with water vapour from various industries into the environment. It is critical to capture/separate targeted gases using appropriate water stable sorbents, meaning that the sorbent materials must be able to sustain the performance during the adsorption process when residual moisture is present. Thus, it is necessary to

consider the effect of the trace amounts of water on the capacity and selectivity of the sorbent material. For instance, Grant Glover *et al.*⁹³ studied the adsorptive removal of several harmful gases including NH₃, CNCl, SO₂, and octane vapour using **M-MOF-74** (M: Zn, Co, Ni, or Mg) in both dry and humid conditions. The experimental breakthrough results revealed that all the prepared MOFs were capable of adsorbing the toxic gases in dry conditions, while in humid conditions the adsorption capability was reduced due to the competitive adsorption of water. The exception was in the case of NH₃ gas, where the decrease in adsorption capacity was negligible, suggesting **ammonia** could be removed by the MOF in both dry and humid conditions.

Moreover, Montoro *et al.* developed a novel MOF,⁹⁴ [**Zn₄(μ₄-O)-(μ₄-4-carboxy-3,5-dimethyl-4-carboxypyrazolato)₃**], which exhibited remarkable thermal, mechanical, and chemical stability. It was found that the synthesised MOF could effectively captures harmful **VOCs** (including Sarin and mustard gas, both are chemical warfare agents), even in competition with ambient moisture. Also, Duan *et al.*⁹⁵ demonstrated that water stable **PCP-33** with significant **C₂H₂ uptake** provides a great potential in applications like purification of natural gas, separation of C₂H₂/CO₂ mixtures, and selective removal of C₂H₂ from C₂H₂/C₂H₄ mixtures at ambient temperature. In addition, Gutov *et al.* reported a highly porous and water stable Zr-based MOF, **NU-1100**, which exhibited very promising gas uptake for **hydrogen and natural-gas-storage** applications.⁹⁶ It was found that the total hydrogen adsorption at 65 bar and 77 K is 0.092 g/g. This renders the material as one of the best performing MOFs for hydrogen storage at low temperatures, not to mention its methane-storage capacities (0.27 g/g at 65 bar and 298 K).

In particular, extensive studies have been carried out regarding **carbon dioxide** due to the strong interest in utilizing MOFs as adsorbents for reducing greenhouse gas emissions. Although water content is often detrimental for CO₂ capture if using MOF materials, there are cases where water has minimal impact. Fracaroli *et al.* used **IRMOF-74-III-CH₂NH₂** for the selective capture of CO₂ in 65% RH.⁹⁷ The experiment results show that this MOF is highly efficient for CO₂ uptake (3.2 mmol of CO₂ per gram at 800 Torr) and, more significantly, able to remove CO₂ from wet nitrogen gas streams with full preservation of the IRMOF structure. Also, Zhang *et al.* highlighted that their developed **Zn-pbdc-12a(bpe)** and **Zn-pbdc-12a(bpy)** exhibit CO₂ uptakes of 98 and 78 cm³/g, respectively, very close to the uptake values prior to water vapour treatment.⁵⁵ Moreover, McDonald and co-workers highlighted that the **mmen-M₂(dobpdc)** (M = Mg, Mn, Fe, Co, Zn) compounds, designated as 'phase-change' adsorbents, possess highly desirable characteristics for the **efficient capture of CO₂**.⁹⁸ The Langmuir-type CO₂ adsorption behaviour can be very well maintained after exposure to water at different temperatures, as shown in Fig. 2.

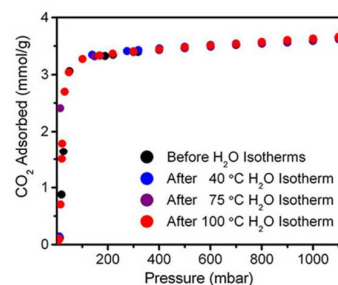


Figure 2. Isothermal adsorption measurements of CO₂ with a sample of mmen-Mg₂(dobpdc) before exposure to water and after water isotherms at 40, 75 and 100 °C.⁹⁸ Reproduced from Ref. 98 with permission, copyright Nature Publishing Group, 2015.

Furthermore, Liao *et al.*⁹⁹ demonstrated that functionalising MOFs by monodentate hydroxide on their pore surfaces could considerably facilitate the **CO₂ capture** performance. The MOF materials – **MAF-X25**, **MAF-X27**, **MAF-X25ox**, **MAF-X27ox** (Fig. 3) – can uptake up to 4.1 mmol cm⁻³ or 13.4 wt% of CO₂ from simulated flue gases even at high RH (82%), and then able to quickly desorb it under mild regeneration conditions (N₂ purge at 358 K). This work represented the best CO₂ capture performance of water stable MOFs reported to that date.

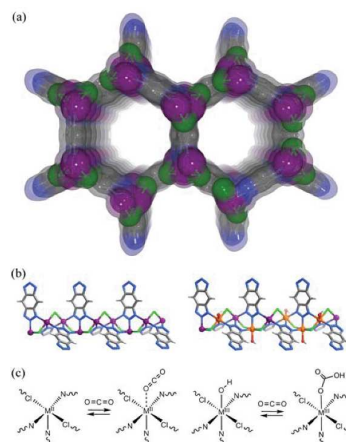


Figure 3. (a) Framework structure of MAF-X25/MAF-X27. Comparison of (b) local coordination structures and (c) CO₂ adsorption mechanisms of MAF-X25/MAF-X27 (left) and MAF-X25ox/MAF-X27ox (right).⁹⁹ Reproduced from Ref. 99 with permission, copyright Royal Society of Chemistry, 2015.

2.2.2 Organics

Further to gaseous phase adsorption, water stable MOFs are as well promising materials for the uptake of organic compounds in liquid form. Typically, the **FMOFs** with super hydrophobicity developed by Yang *et al.* were able to selectively adsorb **C₆-C₈ hydrocarbons** in preference to water.⁶⁹ With the remarkable air and water stability, it was confirmed that FMOFs can be applied in the field of oil spill clean-up and hydrocarbon storage. Also, He *et al.* developed the **MAF-6** with high crystallinity, large surface area, high hydrophobicity and great chemical stability, as shown in Fig. 4.⁵⁰ The MOF can readily adsorb large amounts of **organic**

molecules (methanol, ethanol, C₆–C₁₀ hydrocarbons, etc.), and also separate these organic molecules from water by preferential adsorption. Furthermore, Chun *et al.* developed a hybrid microporous materials with hydrophobic surfaces by coating a water stable MOF, **UiO-66-NH₂**, with microporous organic frameworks (MONs).¹⁰⁰ The resulted MOF@MON hybrid materials demonstrate an excellent performance for adsorption of **toluene** in water.

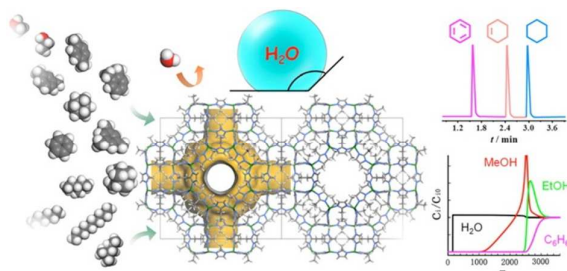


Fig. 4 Exceptional hydrophobicity of a large-pore MAF-6 with organic adsorption/separation capabilities.⁵⁰ Reproduced from Ref. 50 with permission, copyright American Chemical Society, 2015.

In addition, several comparison studies on adsorptive removal of common organic compounds from water were conducted. Xie *et al.*¹⁰² conducted a comprehensive study to screen a series of MOFs for **nitrobenzene (NB) capture** from water. The results suggested that the adsorption capacities of two aluminium-based MOFs, **CAU-1 and MIL-68(Al)**, greatly outperform most of the previously reported porous materials. This was greatly owing to the μ_2 -OH groups in Al–O–Al units of Al-MOFs for the uptake of NB. In addition, the regeneration of CAU-1 and MIL-68(Al) could be fully achieved using methanol without secondary pollution. The great stability and reusability of these MOFs indicate that they are promising adsorbents for efficient capture of organic pollutants from wastewater. In addition, Jin *et al.* investigated three ZIFs (**ZIF-8, ZIF-90 and ZIF-93**) for adsorption of **5-hydroxymethylfurfural (HMF)** from aqueous solution.¹⁰¹ It was found that the equilibrium uptake of HMF increased following the order of ZIF-93 (279 mg g⁻¹) < ZIF-90 (307 mg g⁻¹) < ZIF-8 (465 mg g⁻¹), in accordance with the hydrophobicity of the frameworks. The findings confirm that ZIF-8 can be employed as an effective and reusable adsorbent for HMF recovery from aqueous solution.

Besides common organic compounds, organic dyes in water remains a great issue of concern as they normally are stable, toxic and even potentially carcinogenic, leading to serious environmental, aesthetical, and health problems. Therefore, effective capture of common dye from water is essential and a range of water stable MOFs have been studied and identified as excellent adsorbents for common dye removal. Particularly, owing to the giant cell volume, extra-large pore size, and unique structure characteristics, the water stable MIL-101 has been extensively studied for dye removal.¹¹⁴ Recent work by Leng *et al.*¹⁰⁵ studied the adsorption interaction between **MIL-101** and **uranine dye** in aqueous solution. Further to that, He *et al.* reported a new microporous negatively charged MOF,

[(C₂H₅)₂NH₂]₂[Mn₆(L)(OH)₂(H₂O)₆]-4DEF.⁷⁵ This MOF exhibited a remarkable capability to selectively adsorb and separate the cationic dye (**methylene blue**) through an ion-exchange process. It was found that this ion-exchange-based separation process is highly related to the sizes or charges of organic dyes, and this relationship can be smartly controlled by the structural characteristics of the synthesised MOF.

Moreover, another class of organic compounds nowadays is an essential and indispensable element of our daily life – pharmaceuticals and personal care products (PPCPs). PPCPs are generally produced with long shelf-life to meet the customers' demand, making them highly persistent in the environment even after these products have been spent. Hence, the removal of these emerging contaminants from potable water and aquatic systems remains a critical and urgent issue. For instance, Seo *et al.*¹⁰⁷ applied **UiO-66** to investigate the adsorptive removal of an herbicide, **mecoprop (methylchlorophenoxypropionic acid, MCPP)** from water. Compared with activated carbon, UiO-66 had a very high adsorption rate. Besides, the adsorption capacity of UiO-66 was higher than that of activated carbon especially at low MCPP concentrations. It was proposed that electrostatic and π - π interactions were essential in the adsorption process. Besides, Khan *et al.*¹⁰⁸ has applied **ZIF-8** for the removal of an endocrine disruptor residual – **phthalic acid (H₂-PA)** from aqueous solutions via adsorption. It was found that the adsorption capacity of ZIF-8 framework was much higher than that of a commercial activated carbon and most reported adsorbents. The adsorption was due to an electrostatic interaction between the positively charged surface of ZIF-8 and the negatively charged PA anions; also, acid-base interactions had a favourable effect in the adsorption of H₂-PA especially at low pH conditions. At last, Zhu *et al.*¹⁰⁶ investigated the removal of two representative organophosphorus pesticides, **glyphosate (GP) and glufosinate (GF)**, by **UiO-67**. The abundant Zr–OH groups, resulting from the missing-linker induced terminal hydroxyl groups and the inherent bridging ones in Zr–O clusters of UiO-67 particles, served as natural anchorages for efficient GP and GF capture. Owing to the strong affinity toward phosphoric groups and adequate pore size, the adsorption capacities in UiO-67 were much higher than those of many other reported adsorbents.

2.2.3 Ions

Effective capture of inorganic ions from water is critical for two major reasons. (1) Some metal ions are precious; proper collection and recovery towards these ions can facilitate their applications in industries. (2) Some dangerous ions as serious pollutants can be a major global threat to the environment; removal of these ions from aqueous solution is crucial as they are mostly toxic even at very low concentrations and could lead to serious health effects on human beings. Newly developed MOF structures with great water stability were reported for heavy metal ions removal. For instance, Meng *et al.*⁵³ developed a 3D pillar-layer framework, formulated as **[Zn(trz)(H₂betc)_{0.5}]-DMF**, with uncoordinated carboxyl groups exhibiting exceptional stability. It can effectively and

selectively adsorb Cu^{2+} ions and has been applied as a chromatographic column for separating $\text{Cu}^{2+}/\text{Co}^{2+}$ ions. Moreover, Fang *et al.*¹¹⁵ synthesized two isostructural mesoporous MOFs, PCN-100 and PCN-101, using $\text{Zn}_4\text{O}(\text{CO}_2)_6$ as secondary building units and two extended ligands containing amino functional groups, TATAB and BTATB. The TATAB ligand that comprises **PCN-100** was employed to capture heavy metal ions (Cd^{2+} and Hg^{2+}) by constructing complexes within the pores with a possible coordination mode. In addition, Carboni *et al.*¹⁰⁹ prepared and functionalized stable and porous **phosphorylurea-derived MOFs with the UiO-68 network topology** as novel sorbents to extract actinide elements (**uranium**) from aqueous media. The great extraction efficiency was due to the optimal channel structures and the incorporating functional ligands with great affinity for actinide. Their results indicate that porous MOF materials could play as a good candidate for uranium sorption from nuclear waste and acid mine drainage.

Further to cationic heavy metal ions, anionic species in water could be effectively removed by MOFs as well. Howarth *et al.* applied **NU-1000** to effectively adsorb and remove **selenite and selenate**,¹¹⁰ as well as **sulphate**¹¹¹ from aqueous solutions. Fu *et al.* synthesised two water stable MOFs, **FIR-53 and FIR-54**, to efficiently trap **chromate** inorganic pollutant ions.⁵¹ Moreover, Zhao *et al.*¹¹⁶ conducted a study towards the stability of MOFs in fluoride solutions based on 11 water-stable MOFs: MIL-53(Fe, Cr, Al), MIL-68(Al), CAU-1, UiO-66(Zr, Hf) and ZIFs-7, -8, -9. In particular, the **defluoridation** performance of **UiO-66** was examined, which showed an adsorption capacity that is higher than most of the conventional adsorbents. On the basis of the systemic study, it was suggested that increasing the number of $-\text{OH}$ groups is an efficient strategy to improve the defluoridation performance of MOFs. Further to that, Zhang *et al.*¹¹³ applied a typical aluminium-based MOF, **MIL-96**, for **defluoridation** of drinking water. The results indicated that the defluoridation efficiency of MIL-96 were far superior to that of activated alumina (AA) or nano-alumina (NA).

Besides, another typical anionic pollutant – arsenic – was investigated comprehensively. Wang *et al.* recently reported a superior performance of using Zr-MOF **UiO-66** to **remove arsenic (arsenate) from water**.¹¹² As adsorbents, UiO-66 crystals can function excellently across a broad pH range of 1 to 10, and achieve a remarkable arsenate uptake capacity of 303 mg/g at optimal pH. This adsorption capacity outperforms most of the currently available adsorbents, which can be found in Fig. 5 together with the adsorption mechanism. Similarly, the capability of removing **aquatic arsenic** species was realized by some other water stable MOFs, e.g., **MIL-100(Fe)**⁹², **MIL-53(Fe)**¹¹⁷ and **ZIF-8**¹¹⁸.

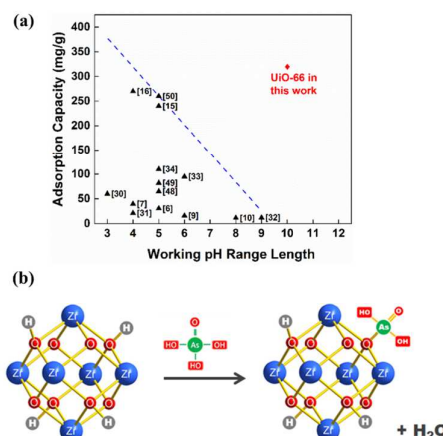


Figure 5. (a) Comparison on arsenic adsorption performance between UiO-66 framework and prevalent adsorbents. (b) Proposed adsorption mechanism of arsenate onto UiO-66 through coordination at hydroxyl group.¹¹² Reproduced from Ref. 112 with permission, copyright Nature Publishing Group, 2015.

2.3 Perspectives

Since the discovery of water stable MOFs and their favourable attributes for adsorption, studies that explored the viability of applying this novel class of materials in various water-related processes have been developed extensively. Rooting from the rational design of crystal structures as well as proper functionalization, MOFs as adsorbents have achieved a great level of both thermodynamic and kinetic performances accompanying great stabilities in applications such as: water retention, selective capture of CO_2 , separation of organic components and removal of anionic species from water solutions.

To go further in the adsorptive applications of water stable MOFs as novel functional porous solids, questions are still remaining on the road to commercialisation. The development of even more powerful MOFs is needed with novel topologies incorporated plenty of effective adsorption sites in unit space. Moreover, whether the material could fully maintain its functions and critical structure across multi-cycles applications remains a questionable challenge. In the past, researchers have mainly focused on studying the hydrothermal stability of pristine MOFs; their stability after the MOFs were put into applications and re-activation needs a more detailed assessment, although a few pioneering studies have been working on this. In addition, prevailing application of certain material normally requires its multifunctionality. To prepare MOF materials with multifunctionality is not easy but definitely feasible due to the customizable and versatile structure provided, which requires significant efforts to take full advantage of the designability of MOFs.

Considered holistically, we have a solid belief that there is a promising future for MOF applications as functional adsorbents. Continuing efforts in both academic and industrial sectors are strongly required in order to achieve a scale-up and cost-effective synthesis and operation process.

3. Membrane separation

Membrane separation has proven to be highly promising in addressing energy and environmental challenges in the past few decades. For instance, membrane-based gas separation offers great potential in practical application, owing to less energy requirement and carbon footprint, as well as easy maintenance and operation. As a new class of inorganic and organic hybrid materials, MOF materials provide new opportunities in separation applications.^{119, 120}

Pioneering studies have looked into the construction of MOF-based thin film. For instance, Guo et al. employed the technique of “twin copper source” to synthesize a copper net supported $\text{Cu}_3(\text{BTC})_2$ membrane.¹²¹ Although $\text{Cu}_3(\text{BTC})_2$ MOF is considered with a limited water stability, its membrane could work under a dry condition with a high permeation flux and excellent permeation selectivity for H_2 .

Nevertheless, the hydrothermal stability of MOFs is always a key issue for their potential capability in separation applications. Industrial feed gas streams normally contain moisture and it is never feasible to completely dry them in order to protect the membrane materials. Therefore, water stable MOFs become a must to introduce MOF membranes in water containing separation applications such as pervaporation, steam separation, desalination, and wastewater treatment (Tab. 2).

Table 2. Membrane separations by water stable MOFs

Water stable MOF based membranes	Process	Flux / Permeance	Rejection / Separation factor / Selectivity	Ref.
ZIF-7	H_2/CO_2 separation	H_2 permeance: $4.5 \times 10^{-8} \text{ mol m}^{-2} \text{ s}^{-1} \text{ Pa}^{-1}$	Separation factor: 13.6	122
ZIF-7 nanosheet	H_2/CO_2 separation	H_2 permeance: 4000 GPU	Selectivity > 200	123
ZIF-90	H_2/CH_4 & H_2/CO_2 separation	H_2 permeance: $2 \sim 2.5 \times 10^{-7} \text{ mol m}^{-2} \text{ s}^{-1} \text{ Pa}^{-1}$	Selectivity: 15.1 & 16.2	124 125
ZIF-8/PMPs	Furfural/water pervaporation	Total flux: $0.90 \text{ kg m}^{-2} \text{ h}^{-1}$	Separation factor: 53.3	126
MIL-53	Dehydration of ethyl acetate by pervaporation	Total flux: $454 \text{ g m}^{-2} \text{ h}^{-1}$	Separation factor: 1317	127
UIO-66	Water softening	Total permeance: $0.14 \text{ L m}^{-2} \text{ h}^{-1} \text{ bar}^{-1}$	Rejection: 86.3% for Ca^{2+} , 98.0% for Mg^{2+} , and 99.3% for Al^{3+}	128
MOF-74/PES	Ultrafiltration (BSA rejection)	Total flux: $80 \text{ L m}^{-2} \text{ h}^{-1}$	BSA rejection: 98%	129

3.1 Membranes based on ZIF-materials

As mentioned in the introduction part, ZIF materials built by azolate ligands, are hydrothermally stable. This renders them to be promising for water included membrane applications. A few ZIF-based membranes^{85, 130, 131} have been prepared (e.g.

ZIF-7,^{122, 123, 132} ZIF-68,¹³⁰ ZIF-69,¹³³ ZIF-71,^{134, 135} ZIF-90,^{124, 125, 136} ZIF-95,¹³⁷ and ZIF-8^{126, 138-141}), and tested for different applications in water systems.

Typically, Li *et al.* reported ZIF-7 based molecular sieve membranes synthesized on asymmetric alumina discs using microwave assisted secondary growth for **hydrogen separation**.¹⁴² Besides a detailed investigation on gas permeations of He , H_2 , N_2 , CO_2 , and CH_4 through ZIF-7 membranes, the hydrothermal stability of the membrane was also tested using an equimolar H_2/CO_2 feed containing 3 mol% steam at 220 °C. It is reported that the ZIF-7 membrane showed a reasonable H_2/CO_2 separation performance and a very high stability for more than 50h of testing as shown in Fig. 6. They observed a slight increase of ~10% on the permeances of H_2 and CO_2 during the stability test, while the separation factor remains unchanged. The increment in the permeances is explained by the removal of some residual polyethylenimine (PEI) components from the seeding procedure in support, indicating an improvement of the membrane performance.

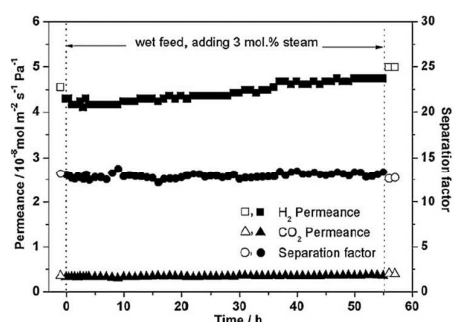


Figure 6. Hydrothermal stability test of the ZIF-7 membrane in separation of an equimolar H_2/CO_2 mixture with adding of 3 mol% steam at 220 °C. Dry feed: empty symbols; wet feed: filled symbols.¹⁴² Reproduced from Ref. 142 with permission, copyright Elsevier, 2010.

Further to that, an ultrathin **2D ZIF-7 like nanosheet membrane** (Fig. 7) was recently prepared by Peng *et al.*¹²³ Benefiting from the exceptional chemical stability of this nanosheet material, which can be obtained via hydrothermal transformation of ZIF-7, no degradation of the membrane performance was observed for various tests up to 400 hours under steam for **H_2/CO_2 separation**. Also, Jin *et al.* developed **2D ZIF-7 like nanosheet mixed matrix membrane** which possesses good hydrothermal stability and high performance as membrane reactor for **bio-furfural production**.¹⁴³

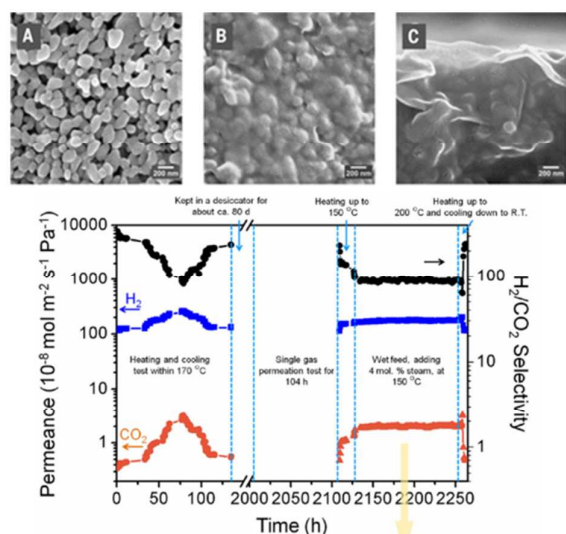


Figure 7. Top: (a) SEM image of bare porous α - Al_2O_3 support, (b) SEM top view, (c) cross-sectional view of the $\text{Zn}_2(\text{bim})_4$ nanosheet layer on α - Al_2O_3 support. Bottom: summary of the long term test of membrane.¹²³ Reproduced from Ref. 123 with permission, copyright The American Association for the Advancement of Science, 2014.

Huang and co-workers have investigated the stability issues of **ZIF-90 membranes** in detail and they recommended the ZIF-90 membrane as a promising candidate for hydrogen production and purification.^{124, 125, 136} In their first study, continuous ZIF-90 molecular sieve membranes were synthesized using 3-aminopropyltriethoxysilane (APTES) as covalent linkers between ZIF-90 and alumina substrate by an imine condensation reaction made possible by the free aldehyde groups in the ZIF-90 framework.¹²⁴ The prepared membrane showed high performance and thermal stability for **H_2/CH_4 separation** in the range of temperatures from 25 to 225 °C. The membrane was also tested for an equimolar H_2/CH_4 mixture containing 3 mol% steam at 200 °C and 1 bar to evaluate its hydrothermal stability, and it showed high stability both in terms of H_2 permeance and H_2/CH_4 selectivity for 24h. ZIF-90 membranes have been suggested for H_2 separation/purification applications at high temperatures due to its thermal and hydrothermal stability. Following these results, the researchers modified the ZIF-90 membrane by covalent post-functionalization using ethanol amine to improve the H_2/CO_2 selectivity.¹²⁵ ZIF-90 has a pore size of 0.35 nm, which is larger than the kinetic diameter of CO_2 (0.33 nm), thus H_2/CO_2 separation is a challenge. Either the compaction of the pore aperture of the ZIF-90 or the reduction of the non-selective transport through invisible intercrystalline defects can be expected as a result of post functionalization, which would substantially enhance the H_2/CO_2 separation selectivity. It was reported that H_2/CO_2 selectivity improved from 7.2 to 16.2 by covalent post-functionalization while the membrane restrained its excellent thermal stability, as well as good stability in the presence of steam at 200 °C, as shown in Fig. 8.

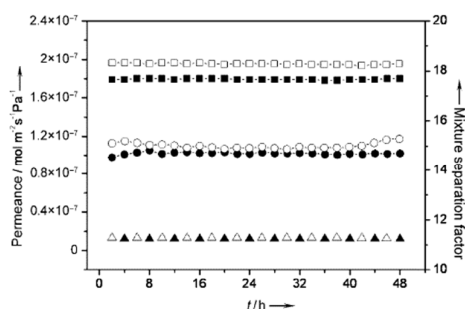


Figure 8. Hydrothermal stability measurement of the imine-functionalized ZIF-90 membrane for the separation of an equimolar H_2/CO_2 mixture upon addition of 3 mol% steam at 200 °C. Open symbols: without steam, filled symbols: with steam; square: H_2 permeance, triangle: CO_2 permeance, circle: separation factor.¹²⁵ Reproduced from Ref. 125 with permission, copyright John Wiley and Sons, 2011.

As one of the most popular ZIFs, **ZIF-8** has also been used for aqueous environments.^{126, 138-141, 144} Yang *et al.* reported ZIF-8/PMPS (PMPS: polymethylphenylsiloxane, a modified silicone rubber) composite membranes for **recovery of furfural (1 wt %) from water** by pervaporation and vapour permeation.¹²⁶ The prepared membrane showed the best pervaporation performance in literature with $0.90 \text{ kg m}^{-2} \text{ h}^{-1}$ total flux and 53.3 separation factor at 80 °C which is owing to the exceptional adsorption selectivity and capacity of ZIF-8 toward furfural molecules. Moreover, as shown in Fig. 9, when it was relied on the hindrance effect of the hydrophobic PMPS on the ZIF-8 fillers, the membrane could stay stable for a long period during pervaporation experiments for the removal of furfural from the dilute aqueous solution. It was found that the furfural permeability was around 125000 Barrer and the furfural/water selectivity was around 11.5 at 80 °C for more than 100 h. The authors suggested MOF filled MMMs as promising membranes for biorefining industry in the future due to the high separation performance and excellent stability of the ZIF-8/modified-silicone-rubber membrane.

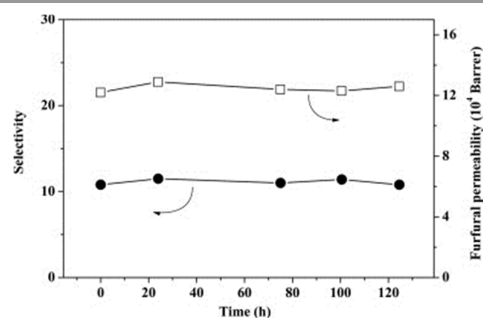


Figure 9. Pervaporation stability test for recovering furfural at 80 °C with 1.0 wt% furfural using ZIF-8-PMPS membranes.¹²⁶ Reproduced from Ref. 126 with permission, copyright Elsevier, 2013.

3.2 Membranes based on other water stable MOFs

Other than ZIF materials, typical water stable MOFs, MIL-53,¹²⁷ UiO-66,¹²⁸ MIL-101¹⁴⁵ and MOF-74¹²⁹ are also used as membrane materials for water related separation applications and tested for hydrothermal stability characteristics.

Continuous **MIL-53 membranes** synthesized by the reactive seeding method on porous alumina support have been reported by Hu and co-workers for the **dehydration of the azeotrope of ethyl acetate (EAC)** aqueous solution by pervaporation.¹²⁷ The high integrity of the membrane was proven by single-gas permeation experiments. The authors reported a flux of $454 \text{ g m}^{-2} \text{ h}^{-1}$ at $60 \text{ }^\circ\text{C}$ with 99 wt % of water concentration in permeate where water-EAC mixture (7 wt % water) passed through the membrane. They explained this finding as the facilitated H_2O transport due to the formed hydrogen bonds between water molecules and hydroxyl groups on the surface of MIL-53. Moreover, in order to evaluate the chemical and mechanical stability of the membranes, they conducted long time pervaporation experiments and MIL-53 membranes showed a high stability for more than 200 h of operation.

Furthermore, Liu *et al.* successfully developed a highly water stable pure-phase zirconium-MOF **UiO-66 polycrystalline membrane** supported on alumina hollow fibres (Fig. 10 Left) for **water softening application**.¹²⁸ The integrity of the membrane was confirmed by single-gas permeation tests, and the membrane exhibited excellent multivalent ion rejection (e.g., 86.3% for Ca^{2+} , 98.0% for Mg^{2+} , and 99.3% for Al^{3+}) on the basis of size exclusion with moderate permeance ($0.14 \text{ L m}^{-2} \text{ h}^{-1} \text{ bar}^{-1}$) and good permeability ($0.28 \text{ L m}^{-2} \text{ h}^{-1} \text{ bar}^{-1} \mu\text{m}$). Besides, the membranes have very stable water filtration performance during the tests around 170 h with different saline solutions at the transmembrane pressure of 10.0 bar (Fig. 10 Right). They claimed that the developed UiO-66 membrane is a promising candidate for water softening due to the high separation performance combined with its outstanding stability.

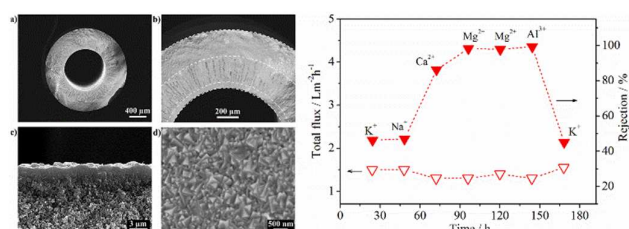


Figure 10. Left: SEM images (a–c, cross section; d, top view) of the alumina hollow fibre (HF) supported UiO-66 membranes. Right: Desalination performance of the UiO-66 membrane. Five different saline water solutions (containing KCl, NaCl, CaCl_2 , MgCl_2 or AlCl_3) with the same concentration (0.20 wt%) were applied as feeds at $20 \pm 2 \text{ }^\circ\text{C}$ under a 10.0 bar pressure difference.¹²⁸ Reproduced from Ref. 128 with permission, copyright American Chemical Society, 2015.

Besides polycrystalline MOF membrane, a wide range of water stable MOFs can be introduced with polymers to form mixed matrix membranes (MMM). Denny *et al.* developed a facile approach to form homogenous **UiO-66/PVDF composite MMMs** with high MOF incorporation, as shown in Fig. 11.¹⁴⁶ These films can be prepared on various substrates and readily delaminated to give durable, large-area, freestanding MMMs with good mechanical stability and flexibility. As the tunability of the component MOF through postsynthetic methods is retained in the MMM, the MMMs can be directly modified in

situ to effect greater functionalities. The study demonstrates that MMM can be a platform to formulate water stable MOFs into an easily handled and readily usable form.

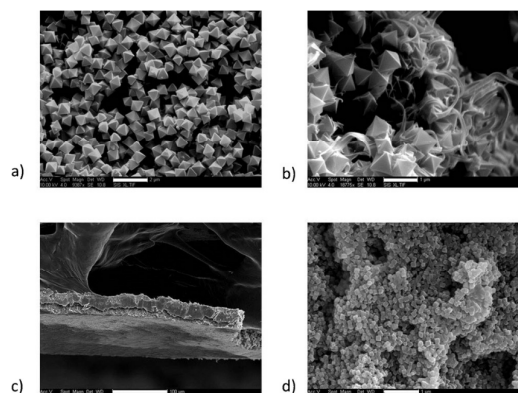


Figure 11. SEM images of UiO-66 MMM: (a) UiO-66 MMM showing MOF microcrystal structure. (b) Torn edge of UiO-66 MMM, showing both the UiO-66 particles and PVDF polymer fibres. (c) Cross-section of UiO-66 MMM showing uniform thickness. (d) Higher magnification of the cross-section, showing densely packed UiO-66 particles in the MMM interior.¹⁴⁶ Reproduced from Ref. 146 with permission, copyright John Wiley and Sons, 2015.

In another MMM study, Sotto and co-workers used Zn- and Co-containing **MOF-74** materials and ZnO as additives in polyethersulfone (PES) to develop composite ultrafiltration membranes using phase inversion induced by the immersion precipitation technique.¹²⁹ Before membrane preparation, the stability of MOF-74 was studied in the synthesis media of polymeric membranes, and showed a high structural stability. Due to the higher pore size, porosity and hydrophilicity of prepared composite membranes, they showed higher water permeability than neat PES membranes. Moreover, **bis(trimethylsilyl)acetamide (BSA) rejections** by the composite membranes were significantly higher than the neat PES membranes. After the stability of the membranes was tested by various cycles of BSA solution filtration, the authors suggested that these MMMs are promising candidates for water purification purposes.

3.3 Perspectives

To sum up, pioneering results in this field have been reported for membrane fabrication on the basis of water stable MOF materials. The majority of them could perform quite well in processes containing water content such as gas separation, pervaporation and pressure-driven filtration.

However, in our opinion, the MOF membrane studies are still in their primitive stage. There is still a long way to go for water stable MOF membranes to be applied in industrial practice. We can see from the currently reported literature that the duration of respective stability tests on the developed MOF membranes only last for a few to hundreds of hours. It is inevitable that a much longer-term stability test is required for the validity of their corresponding performances; not to mention that the overall performance of MOF membranes still

needs enhancing in order to compete with the commercial ones.

Looking forward, with the emergence of more and more water stable MOFs offering versatile architectures and customizable functional groups, membrane researchers are fortunate that a number of potentially qualified materials are ready for various membrane applications. They can work on polycrystalline MOF membranes and MOF mixed matrix membranes, both of which possess a great potential as next-generation membranes to expand the membrane database or even overtake the commercially available membranes in some application areas.

4. Sensing

The application of water stable MOFs in sensing normally falls in two regions: the detection of water, and the identification of specific target from water media (Tab. 3). Chemical analysis for the water content is essential not only for chemical industries producing anhydrous chemicals but also for oil and petroleum industries in which water is regarded as contaminant and impurity. Besides, accurate determination of particular compounds present in water is important taking water safety concern as one representative example. With the prerequisite of hydrolytic stability, it is certain that MOFs could provide a platform in the area of fast and reliable sensors, since both the organic ligands (containing aromatic or conjugated moieties) and metal components (e.g. lanthanides) could contribute to photoluminescence as well as electrochemical sensing.¹⁴⁷ This further extends the scope of MOF applications, and would lead to the development of commercial sensing devices.

Table 3. Sensing applications of water stable MOFs

Water stable MOF	Sensing targets	Water presence	Ref.
NH ₂ -MIL-125(Ti)	Water	Sensing target	148
HKUST-1	Water	Sensing target	149
ZIF-8	Water	Sensing target	150
Cu(I)-MOF	Water and formaldehyde species	Sensing target	151
AEMOF-1	Water	Sensing target	152
CAU-10	Water	Sensing target	176
PCN-222	H ⁺	Water solution	153
UiO-66-NH ₂	H ⁺	Water solution	154
InPCF-1	Methylviologen and Cu ²⁺ ions	Water solution	38
Cd-EDDA	Hg(II)	Water solution	155
[Cd ₂ L ₂]-NMP-MeOH	Cu ²⁺	Water solution	156
Eu/UiO-66-(COOH) ₂	Cd ²⁺	Water solution	157
Eu/CPM-17-Zn	Cd ²⁺	Water solution	158
Eu/MIL-53-COOH(Al)	Fe ³⁺	Water solution	159
[Ln(HL)(H ₂ O) ₂] _n ·2H ₂ O	Fe ³⁺	Water solution	33
Eu ³⁺ @MIL-124	Fe ³⁺ and Fe ²⁺ ; Cr ₂ O ₇ ²⁻ and acetone	Water solution	160

[(Tb(L ₁) _{1.5} (H ₂ O))·3H ₂ O] _n	Fe ³⁺ and Al ³⁺ ; TNP	Water solution	36
[Tb(L)(OH)]·x(solvent)	TNP	Water solution	35
bio-MOF-1	TNP	Water solution	161
UiO-68-NH ₂	TNP	Water solution	162
Zn ₃ (btc) ₂ ·12H ₂ O	Alcohol gas	Co-existence	163
[Zn ₄ (Hbpvp) ₂ (BTC) ₃ (HCOO)(H ₂ O) ₂ ·4H ₂ O	2,4-dinitrophenol and <i>p</i> -benzoquinone	Water solution	164
Cu-bipy-BTC/Carbon nanotube	Hydrogen peroxide	Water solution	165
BFMOF-1	H ₂ S	Water-based biological and environmental assays	166
MIL-121	Hippuric acid	Urine	39

4.1 Detection of water

The development of efficient sensors for the detection of water is highly desirable in various industries, for instance, the accurate determination of water content in ethanol is of high importance for the fuel, alcoholic beverage, and solvent industries. Moreover, since industrial gases are easily contaminated with water moisture during stages like production, transfer or use, while trace water in the industrial gases can cause severe quality problems, it is important to monitor and to control trace water levels in industrial gases.

Some sensors for **water detection** were developed based on functional thin films of water stable MOFs. One typical setup reported by Zhang *et al.* using **NH₂-MIL-125(Ti)**.¹⁴⁸ The NH₂-MIL-125(Ti) humidity sensor was fabricated by coating the nano-size materials on interdigitated electrodes, as shown in Fig. 12. The humidity sensor based on NH₂-MIL-125(Ti) shows good linearity of relative humidity (11-95 % RH), as well as fast response and recovery time.

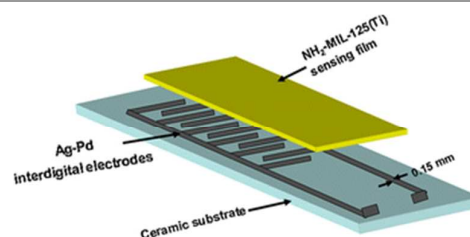


Figure 12. Schematic representation of electric-based MOF sensor.¹⁴⁸ Reproduced from Ref. 148 with permission, copyright Springer, 2013.

Furthermore, several colorimetric sensors were also reported. In recent studies, Li *et al.* fabricated ultrathin **ZIF-8** coated monolayer colloidal crystals and applied for highly efficient vapour sensing.¹⁵⁰ Next, Yu *et al.* developed a porous **Cu(I)-MOF** constructed from Copper(I) iodide and 1-benzimidazolyl-3,5-bis(4-pyridyl)benzene.¹⁵¹ This Cu(I)-MOF can work as a highly sensitive naked-eye colorimetric sensor to successively **detect water and formaldehyde species** at very low concentrations. Moreover, Douvali *et al.* presented a Mg(II) MOF, **AEMOF-1**, featuring the remarkable capability to

rapidly **detect traces of water** in various organic solvents.¹⁵² This was achieved through an unusual turn-on luminescence sensing mechanism, in contrast to the most common luminescence quenching method. The MOF material can selectively capture water molecules and confine them in its pores building up high local concentrations, which consequently amplify the emission properties of the bridging ligand.

In addition, Weiss *et al.* reported that three mixed-linker CAU-10 type MOFs, $[\text{Al}(\text{OH})(1,3\text{-BDC-X})_n(1,3\text{-BDC-SO}_3\text{H})_m]$ with $X = \text{H}, \text{NO}_2$ or OH , are potential candidates as sensor-active materials in **humidity sensing**.^{167, 168} The authors developed a setup accommodating the response of CAU-10 samples under exposure to different RH in air by impedance spectroscopy. The results prove that the MOFs are qualified for functional layers of capacitive humidity sensors. Since the prepared MOFs possess a greater hydrothermal stability than that of many commonly used polymers, they can be a new generation humidity sensors, to be used in high-temperature (up to 350 °C).

4.2 Detection of targets in water

Researchers strategically employed the unique features of different water stable MOFs, and came up with a bunch of effective sensors to identify different targets from water media. These targets include proton concentration for pH sensing, other inorganic ions, and organic components especially environmental pollutants. It has been proven that water-stable MOFs with specific functionalities hold a great potential as sensing materials for determining specific targets in water.

First of all, several pH-dependent fluorescent studies using water stable MOFs as materials were reported. Deibert *et al.* reported that a distinct reversible colorimetric and fluorescent “turn-off-turn-on” **pH response** can be produced by the water stable **PCN-222** with the incorporating H_2tcpp moiety.¹⁵³ More importantly, it was shown that the material has the advantage of full reversibility and reusability that outperforms its molecular analogues, and can act as a luminescent or colorimetric solid-state sensor for the low pH values (0-3) across a wide pH range. Furthermore, Aguilera-Sigalat *et al.*¹⁵⁴ managed to apply a colloidal water-stable MOF (**UiO-66-NH₂**) as a broad-range (pH 1-9) fluorescent **pH sensor**. Further to that, by application of a post-synthetic modification (PSM) diazotisation strategy, the author synthesized a new material, UiO-66-N=N-ind, which provides an increased chemical stability and enhanced sensing up to pH 12.

Besides pH sensing, typical ionic targets can be efficiently detected by water stable MOFs as well. Dan *et al.*³⁸ developed a highly stable indium phosphonocarboxylate framework, **InPCF-1**, as a multifunctional sensor for **methylviologen** and **Cu²⁺** ions. Sensing of inorganic mercury has been covered by Wu *et al.*¹⁵⁵ They developed a Cd-MOF, **Cd-EDDA**, with dual-emission signals as a MOF-implicated ratiometric sensor for **Hg(II)** in pure water with a fast response, high selectivity and sensitivity. Besides, another Cd-MOF for sensing applications was carried out by Shao *et al.*¹⁵⁶ They synthesised and

characterised a new water-stable 3D MOF, **[Cd₂L₂]-NMP-MeOH**. The luminescent studies indicate that this MOF has significantly high specific, selective and sensitive quenching effect toward **Cu²⁺**, implying that it could be used as a luminescent probe for the detection of **Cu²⁺**.

Further to that, more responsive sensors can be developed through the incorporation of lanthanide groups into a water stable framework. Typically, a couple of studies were with respect to **Cd²⁺** detection. Liu *et al.* encapsulated **Eu³⁺** ions to partial replace the transition-metal clusters in the channels of **CPM-17-Zn** nanocrystals (Fig. 13).¹⁵⁸ The **Eu³⁺** functionalized MOF hybrid system provides an excellent luminescence property and photo-stability in aqueous environment. As a highly selective and sensitive sensor, the nanocrystals can be used to detect **Cd²⁺** in aqueous solution. The good fluorescence stability, low detection limit and broad linear range in aqueous environment render this probe to be promising for intracellular sensing and imaging of **Cd²⁺**.



Figure 13. Synthetic procedure of CPM-17-Zn-Eu and its fluorescent enhancement by Cd^{2+} .¹⁵⁸ Reproduced from Ref. 158 with permission, copyright Elsevier, 2015.

Moreover, multi-functional MOF sensors with both inorganic and organic sensing capabilities were synthesised by introducing **Eu³⁺** cations. Xu *et al.* prepared a layerlike MOF (**MIL-124**) as a parent compound to encapsulate **Eu³⁺** cations by one uncoordinated carbonyl group in its pores.¹⁶⁰ The **Eu³⁺**-incorporated sample (**Eu³⁺@MIL-124**) shows excellent luminescence and good fluorescence stability in water or other organic solvents. It was found that the complex **Eu³⁺@MIL-124** is highly selective and sensitive for the detection of **Fe³⁺** and **Fe²⁺** ions through fluorescence quenching of **Eu³⁺**, as shown in Fig. 14. In addition, when **Eu³⁺@MIL-124** was immersed in the different anions solutions and organic solvents, it also shows highly selective for **Cr₂O₇²⁻** and **acetone**. Besides, Song *et al.* obtained a hydrothermally robust, luminescent microporous **Eu-based MOF sensor**.⁶⁴ It is capable of sensing small organic **acetone** molecules and inorganic ions (**Cu²⁺**, **NO₃⁻**, **F⁻**, **Cl⁻**, and **Br⁻**); and unprecedentedly it can discriminate among the homologues and isomers of aliphatic alcohols as well as detect highly explosive **2,4,6-trinitrophenol (TNP)** in water or in the vapour phase (Fig. 15). In addition to Eu-functionalized MOF sensors, another multifunctional sensing MOFs was introduced by Cao *et al.*³⁶ It is a water-stable luminescent Tb-based MOF, **[(Tb(L₁)_{1.5}(H₂O))·3H₂O]_n (Tb-MOF)**, with rod-shaped secondary building units (SBUs) and honeycomb-type tubular channels.

The high green emission intensity and the microporous nature of the Tb-MOF lead to its potential use as a luminescent sensor. The authors identified that this Tb-MOF can selectively sense Fe^{3+} and Al^{3+} ions from mixed metal ions in water through different detection mechanisms. Furthermore, it also exhibits high sensitivity for TNP in the presence of other nitro aromatic compounds in aqueous solution by luminescence quenching experiments.

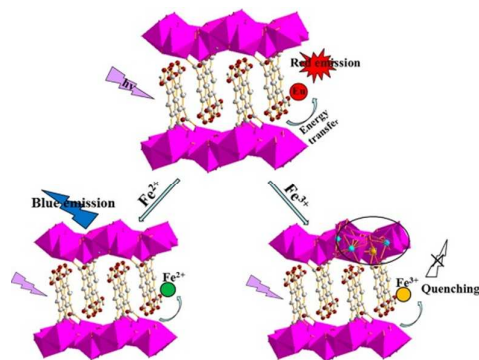


Figure 14. Schematic illustration of luminescence quenching mechanism of Eu^{3+} @MIL-124 by Fe^{3+} and Fe^{2+} ion.¹⁶⁰ Reproduced from Ref. 160 with permission, copyright American Chemical Society, 2015.

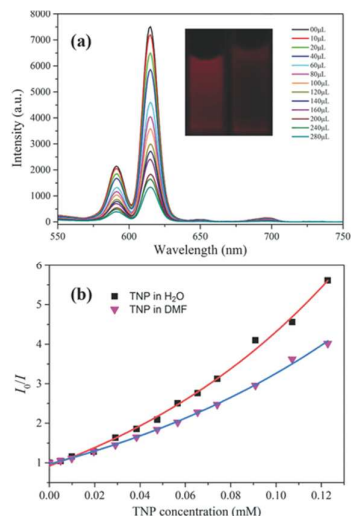


Figure 15. (a) Emission spectra of Eu-MOF dispersed in water with incremental addition of TNP aqueous solution. Inset shows the photograph of original fluorescence (left) and quenching fluorescence (right). (b) Stern–Volmer plots of I_0/I versus the TNP concentration in DMF and water.⁶⁴ Reproduced from Ref. 64 with permission, copyright John Wiley and Sons, 2014.

As TNP is a widely-recognized harmful environmental contaminant in water media, prompt and selective detection of nitro explosives in the aqueous phase is in great demand with respect to the homeland security and environmental concerns. Another TNP probe was envisioned by Joader *et al.* using a hydrolytically stable 3D luminescent MOF, **bio-MOF-1**.¹⁶¹ The excellent hydrolytic stability allows it to be used in water, and significantly large pore windows allow easy diffusion of analytes inside the MOF channels. The developed compound can sense TNP exclusively even in the presence of

other nitro-compounds. Also, Nagarkar *et al.* reported a chemically stable porous MOF, **UIO-68-NH₂** with a Lewis basic free amine functionality as a pendant recognition site for the selective and sensitive detection of TNP in the aqueous phase.¹⁶² The high selectivity was observed even in the presence of competing nitro-analytes in the aqueous phase. This unprecedented selectivity is ascribed to electron-transfer and energy-transfer mechanisms as well as electrostatic interactions between TNP and the MOF.

Besides TNP, water stable MOFs were applied to detect other organic components. Dong *et al.* developed a highly sensitive electrochemical sensor for the determination of **2,4-dichlorophenol (2,4-DCP)** based on **HKUST-1** modified carbon paste electrode.¹⁶⁹ The sensor can be applied for the determination of 2,4-DCP in reservoir raw water samples with satisfactory results. Besides, Pentylala *et al.* synthesised the compound **Zn₃(btc)₂·12H₂O (Zn-btc)**.¹⁶³ This Zn-btc framework is able to deliver the **alcohol gas** sensing interaction based on the exchange of Zn-coordinated water to alcohol molecules. Also, Shi *et al.* reported a fluorescent Zn(II)-supported MOF, **[Zn₄(Hbvpv)₂(BTC)₃(HCOO)(H₂O)₂·4H₂O]** through the solvothermal reactions.¹⁶⁴ The compound exhibits a high sensitivity and a low limit of detection for both **2,4-dinitrophenol** and **p-benzoquinone** in aqueous solutions. Its fluorescent intensity recovers upon removal of analytes, making it a promising recyclable dual-targeted luminescent probe. In addition, **[Cd₂(TBA)₂(bipy)(DMA)₂]** was synthesized by Wang *et al.* under solvothermal conditions, demonstrating a great hydrothermal stability.⁶⁶ It was successfully applied to detect different volatile organic solvent molecules, with the best quenching behaviour by **acetone**. Furthermore, Liu *et al.* developed a stable 3D coordination polymer, **[Eu₃(bcbp)₃(NO₃)₇(OH)₂]_n**, by the solvothermal reaction.¹⁷⁰ This MOF exhibits a strong red-light emission at ambient temperature. Due to the presence of the electron-deficient bipyridinium moiety in the conjugation, this emission is selectively quenched by electron-rich **organic amine compounds** with high sensitivity and exhibits a prominent visual colour change.

Furthermore, Zhou *et al.* synthesised a Cu(II)-based MOF (**Cu-bipy-BTC**) and then immobilized on multiwalled carbon nanotubes.¹⁶⁵ The prepared composite was applied in a non-enzymatic **hydrogen peroxide** biosensor. The sensor showed good electrocatalytic activity toward hydrogen peroxide, as well as good stability and repeatability. More importantly, the sensor shows great accuracy for the determination of hydrogen peroxide in water samples. Moreover, Cui *et al.* developed and characterised an amphoteric MOF, **BFMOF-1**,¹⁶⁶ which is composed of a backfolded linker unit which has a soft core and rigid arms. The distinct colour changes of BFMOF-1 in response to **H₂S** giving rise to potential sensing applications. As shown in Fig. 16, a light but distinct red colour quickly developed even when H₂S was present at trace level; and the colour darkens systematically at higher concentrations. What is more, the BFMOF-1 solid is insoluble in water and is readily applicable in monitoring H₂S in water-based biological and environmental assays.

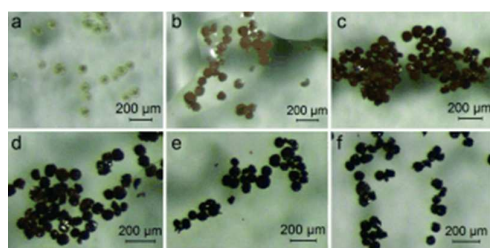


Figure 16. H₂S sensing by the colour change in BFMOF-1.¹⁶⁶ Reproduced from Ref. 166 with permission, copyright John Wiley and Sons, 2014.

4.3 perspectives

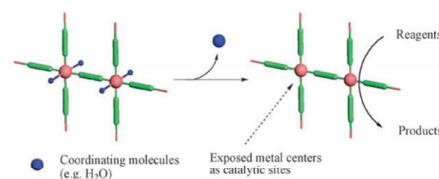
In the past decade, a variety of MOF materials have been put into the application as sensors despite their water stability. For example, Kumar et al. synthesized a MOF-5 based luminescent material for the sensing of nitro group.¹⁷¹ Going beyond, much more rigorous studies were conducted for the sensing applications by water stable MOFs. Respective targets including water, inorganic and organic compounds were examined, which forms a comprehensive picture in the field of sensing. In particular, the detection of explosive molecules is a highlight among the sensing application of water stable MOFs. Quick and precise response to the life-threatening active substances could help save human lives and protect environment. Compared with other sensory materials like some polymers, MOFs have great advantages as mentioned previously. Typically, polymeric sensors would lose their emission properties at elevated temperatures or extreme conditions, whereas sensors based on the ultra-stable MOFs would not have this problem.

However, to produce MOF-based sensor in commercialised applications, continuing efforts are on demand to streamline the synthesis and functionalization process of raw materials. Also, how to incorporate the active sensing MOFs into a portable detection device requires further engineering and smart designs. Ultimately, a facile and cost effective protocol must be presented in industrial developments.

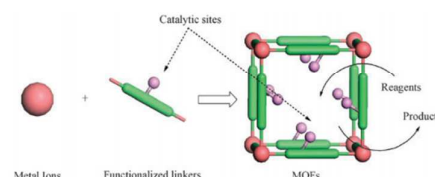
5. Catalysis

MOF materials generally provide substantially high porosity, which render adequate spaces for the incorporation of functional groups. As shown in Fig. 17, strategic designs towards the MOFs can result in promising catalysts for various reactions.¹⁷² This makes MOFs potential candidates for the application as catalysts. However, in order to function effectively in reactions where water is involved, sufficient hydrothermal stability of the catalyst is vitally important. Water sensitive materials would suffer from the detrimental effects or even severe structural degradation due to the presence of water in the reactive environment. Hence, catalysts based upon water stable MOFs stand out as they not only take advantages of the desirable features of MOF materials like tunability and regular catalytic sites, but also are capable of remaining robust and effective throughout the

process. The benchmark examples reported in recent years are listed in Tab. 4.



Scheme 1 Coordinatively unsaturated metal connecting points as active catalytic sites.



Scheme 2 Incorporation of active catalytic sites into the bridging ligands of MOFs.

Figure 17. Two schemes showing potential catalytic sites within MOF structures.¹⁷² Reproduced from Ref. 172 with permission, copyright Royal Society of Chemistry, 2009.

Table 4. Catalysis applications of water stable MOFs

Water stable MOF	Catalytic reaction	Yield	Ref.
NENU-500	Hydrogen evolution reaction	-	173
Co-ZIF-9	Oxygen evolution reaction	-	215
Al ₂ (OH) ₂ TCPP-Co	Reduction of carbon dioxide	76% selectivity for CO	174
Al-MIL-101-NH-Gly-Pro	Asymmetric aldol reaction	80% in asymmetric aldol reaction	175
UiO-66-CAT	Oxidation of alcohols to ketones	99% in alcohol oxidation for a range of substrates	176
Pt/UiO-66	Aqueous reaction in 4-nitrophenol reduction	100% conversion	177
MOF-808 (6-connected)	Hydrolysis of dimethyl 4-nitrophenyl phosphate (DMNP)	100% conversion	26
NU-1000	Hydrolysis of DMNP	100% conversion	178
MOF-808-2.5SO ₄ [Zr ₆ O ₅ (OH) ₃ (BTC) ₂ (SO ₄) _{2.5} (H ₂ O) _{2.5}]	Esterification	80% conversion	179
POM-ionic-liquid-functionalized MIL-100	Esterification of oleic acid with ethanol	94.6% conversion of oleic acid	180
HPW@MIL-101	Hydrolysis of ethyl acetate; esterification of acetic acid with n-hexanol	15% conversion in ethyl acetate hydrolysis in water; 60% yield of hexyl acetate	181
Sulphated MIL-53	Esterification of n-butanol and acetic acid	-(TOF: 1.04 min ⁻¹)	182
MIL-101(Cr)-NO ₂	Acetalization of benzaldehyde in methanol	99% conversion	183

NENU-1/12-tungstosilicic acid	Dehydration of methanol to dimethyl ether	67% of ethyl acetate	184
-------------------------------	---	----------------------	-----

5.1 Water as reaction source

There are many reactions involving water as the source. Numerous homogeneous and heterogeneous water oxidation and reduction catalysts have been developed with the intention of accessing low energy pathways to clean oxygen and hydrogen. With respect to this, Meyer *et al.* comprehensively summarised the applications of water stable MOFs as either participants or solid supports in catalytic water splitting.¹⁸⁵ In order to participate in water splitting, a MOF should demonstrate stability under aqueous conditions and may also need to tolerate other factors like solution pH. Representative frameworks that could support the rigours of water splitting include: UiO-66 (Zr) and UiO-67 (Zr),^{19, 186} MIL-100 (Cr),¹⁸⁷ MIL-101 (Al and Cr),^{18, 188} MIL-53 (Al and Cr),^{189, 190} MIL-125 (Ti),¹⁹¹ ZIF-8 (Zn),⁴³ certain PCNs (Zr-porphyrins),¹⁹² and SIM-1 (Zn).¹⁹³ Specifically, **UiO-66**, **UiO-67**, **MIL-101** and **MIL-125** materials appear most frequently in the applications of **water oxidation and reduction catalysis**.

In particular, electrocatalytic reduction of water to molecular hydrogen via hydrogen evolution reaction is a simple and effective method for clean and renewable energy source production. Aqueous stability of the catalysis used in this reaction is critical to improve the efficiency of the system. Qin and co-workers suggested using two novel polyoxometalate (POM)-based MOFs, **NENU-500** and **NENU-501**, as electrocatalysts to be used in **hydrogen evolution reaction** to generate hydrogen from water under acidic conditions.¹⁷³ Both showed remarkable performance owing to the combination of the redox activity of a POM unit and the porosity of a MOF. Furthermore, Wang *et al.*^{194, 195} introduced a new type of heterogeneous water oxidation catalyst by assembling cobalt ions and benzimidazole ligands to form a crystalline microporous **Co-ZIF-9**, which can effectively electrocatalyze the **oxygen evolution reaction** in a wide pH range (under both acidic and alkaline conditions).

5.2 Water as reaction solvent/product

Moving on, water has as well been used as the solvent in catalytic reactions (e.g. ester hydrolysis) due to the availability, environmental friendliness and safety. For such cases, water stable MOFs provide an appealing platform to the development of an ideal catalytic process. Also, in the reactions that water is produced as the result (e.g. esterification), it is necessary that catalysts could stay serviceable throughout the reaction process where water is generated as product. Otherwise, if water cannot be removed in time, it would disrupt the catalysts, causing the reaction efficiency deteriorates sharply. Classic examples were summarised by Dhakshinamoorthy *et al.* in 2014.¹⁹⁶ On top of that, much more newly developed water stable MOFs have been successfully applied in catalytic reactions with water as medium/product.

Kornienko *et al.* demonstrated the applicability of MOF ($\text{Al}_2(\text{OH})_2\text{TCPP-Co}$) catalyst for the efficient and selective **reduction of carbon dioxide** to carbon monoxide in aqueous electrolytes.¹⁷⁴ It was observed that a selectivity for CO production in excess of 76% and stability over 7 h with a per-site turnover number (TON) of 1400. This was achieved via the redox-accessible catalytic centres, where Co(II) is reduced to Co(I) during reaction. In addition, Bonnefoy *et al.* studied the application of chiral peptide MOFs as catalysts in the asymmetric aldol reaction between acetone and 4-nitrobenzaldehyde.¹⁷⁵ This reaction requires the presence of a proton source, water in this case, to proceed efficiently. Since the MIL-101 cavity is large enough to accommodate both the anchored organocatalyst and the reactants, the authors functionalized this platform using 15 mol % of proline moieties (Fig. 18) at room temperature in the presence of water. At the end, it was found that **Al-MIL-101-NH-Gly-Pro** catalysed the **asymmetric aldol reaction** giving the product 4-hydroxy-4-(4-nitrophenyl)-butan-2-one with 25% enantioselectivity. A leaching test showed that no active proline moieties are released in the solution during the course of the reaction.

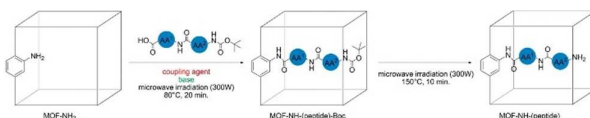


Figure 18. Peptide grafting process into MOFs for specific catalysis application.¹⁷⁵ Reproduced from Ref. 175 with permission, copyright American Chemical Society, 2015.

Moreover, Fei *et al.* developed a reusable oxidation catalyst by introducing Cr-monocatecholato species into the robust **UiO-66** framework by post synthetic exchange strategy.¹⁷⁶ As shown in Fig. 19, it is effectively applied for catalysing the **oxidation of alcohols to ketones** using, for example, H_2O_2 in aqueous solution as the oxidant, giving water as the sole by product. Compared to other synthetic catalysts, the MOF-based catalysts reported in their study are completely recyclable and reusable, which render them attractive catalysts for the green chemistry process. Besides, Zhang *et al.* introduced the noble-metal nanoparticles (NPs) into the carboxylate-MOFs.¹⁷⁷ As shown in Fig. 20, the obtained **Pt/UiO-66** composites exhibited excellent shape-selective catalytic properties in **olefin hydrogenation**, **aqueous reaction in 4-nitrophenol reduction**, and enhanced molecular diffusion in CO oxidation.

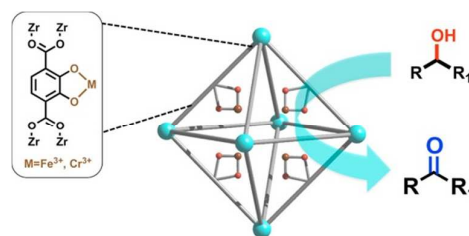


Figure 19. Synthesis of UiO-66-CAT as efficient and green alcohol oxidation catalyst.¹⁷⁶ Reproduced from Ref. 176 with permission, copyright American Chemical Society, 2014.

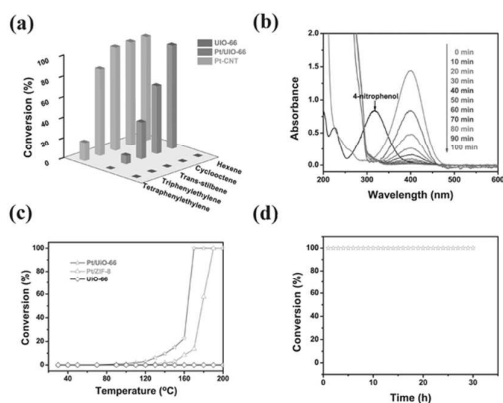


Figure 20. Catalytic performance of Pt/UiO-66 composites. (a) Hydrogenation of olefins catalyzed by Pt/UiO-66 composite. (b) UV-vis spectra showing gradual reduction of 4-nitrophenol over Pt/UiO-66. (c,d) CO oxidation catalysis by Pt/UiO-66: conversion versus temperature (c) and at 180 °C versus time (d).¹⁷⁷ Reproduced from Ref. 177 with permission, copyright John Wiley and Sons, 2014.

Furthermore, Moon *et al.* used **MOF-808 (6-connected)** as an effective catalyst for the **hydrolysis reaction of nerve-agent simulant, dimethyl 4-nitrophenyl phosphate (DMNP)**, in aqueous buffer solution.²⁶ The highest hydrolysis rates was found compared to all MOFs reported to that data. Another study by Mondloch *et al.* carried out **catalytic hydrolysis of DMNP** using **NU-1000** in an aqueous N-ethylmorpholine buffered solution at pH 10.¹⁷⁸ The fastest known decomposition rate of a phosphate ester nerve agent simulant was noted compared to other MOF catalysts. Also, NU-1000 is completely recyclable for the reaction over three runs.

Next, when water is produced as reaction product, another catalysis study using MOF-808 was carried out by Jiang *et al.*¹⁷⁹ They reported the superacidity in a sulfated MOF by treating the microcrystalline form of MOF-808 with aqueous sulfuric acid to generate **MOF-808-2.5SO₄[Zr₆O₅(OH)₃(BTC)₂(SO₄)_{2.5}(H₂O)_{2.5}]**. This material was found to be catalytically active in various acid-catalyzed reactions including **esterification**. Besides, Wan *et al.* the **POM-ionic-liquid-functionalized MIL-100** and used it in biodiesel production through the **esterification of oleic acid with ethanol**.¹⁸⁰ It was found that the conversion of oleic acid could reach 94.6% at optimal conditions, indicating a great catalytic activity. Moreover, the catalyst could be easily recovered and reused six times, without obvious leaching of the active component.

In addition to esterification catalysis, porous **2-nitro-, 2-amino-, and nonfunctionalized MIL-101(Cr)** were studied by Herbst *et al.* as heterogeneous catalysts for **diacetal formation of benzaldehyde and methanol (B-M reaction)** and other aldehydes and alcohols, where water is formed in the equilibrium reaction (Fig. 21).¹⁸³ The authors reported that the catalytic activity increased with surface area within different samples of nonfunctionalized MIL-101, while the activity decreased in the order MIL-101-NO₂ > MIL-101 > MIL-101-NH₂ for the functionalized samples. The highest catalytic performance was reported as 99% conversion in the B-M

reaction within 90 min and turnover numbers of 114 for MIL-101-NO₂.

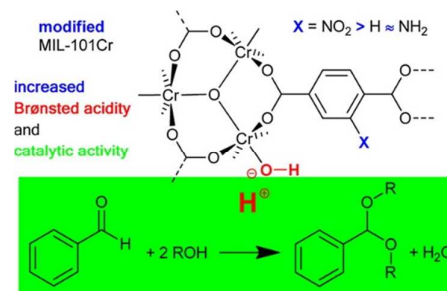


Figure 21. Brønsted acidity in functionalized MIL-101(Cr) MOFs for efficient heterogeneous catalysis in the condensation reaction of aldehydes with alcohols generating water.¹⁸³ Reproduced from Ref. 183 with permission, copyright American Chemical Society, 2014.

Besides, Liang *et al.* reported the development of a crystalline catalyst based on a porous copper-based metal-organic framework (**NENU-1**) and 12-tungstosilicic acid (Fig. 22).¹⁸⁴ This crystal catalyst has both the Brønsted acidity of 12-tungstosilicic acid and the Lewis acidity of the NENU-1, and thus has high density of accessible acid sites. Its catalytic activity was fully assessed in the **dehydration of methanol to dimethyl ether**. Since water is one of the products of methanol dehydration, the presence of excess water may decrease the methanol conversion efficiency. Moreover, water can compete with methanol for the Lewis acid sites on the catalyst, leading to the reduced Lewis acid activity. With respect to this NENU-1 based catalyst, high catalytic performance was maintained even when the crude methanol with 20 wt% water was fed, demonstrating a great water resistance. This advantage is attributed to the high density of Brønsted acid sites available,¹⁹⁷ whereas water only reduces the activity of Lewis acid sites but has little effect on Brønsted acid sites. Therefore, cheaper crude methanol with a higher water content can be used as raw material instead of expensive anhydrous methanol, when the NENU-1 based catalyst is used as the catalyst for DME production. Moreover, the high catalytic activity in the presence of excess water also allows this catalyst to be used in the syngas-to-DME process, which is another important industrial process involved in DME production.

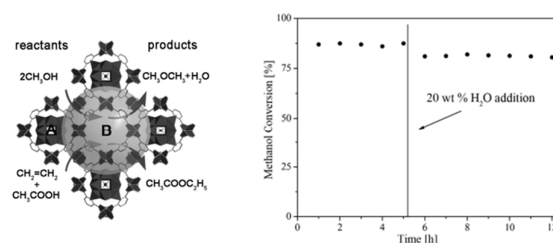


Figure 22. Left: crystalline catalyst based on a porous Cu-MOF and 12-tungstosilicic acid. Right: water addition effect over NENU-1 based catalyst. Anhydrous methanol was fed at the first 5 h, and then methanol with 20 wt% water was fed instead (vertical line).¹⁸⁴ Reproduced from Ref. 184 with permission, copyright John Wiley and Sons, 2014.

5.3 Perspectives

Going through the studies that applied water stable MOFs for catalytic activities, we have seen many successful cases being introduced but clearly there is still a long way to go for complete understanding. Since the research in this field is in its infancy and a range of reactions have not yet been studied with water stable MOFs, numerous opportunities are awaiting ahead. After all, it is undeniable that MOFs feature a series of merits for catalytic activities, especially its major limitation – lack of structural stability has been significantly overcome now.

Therefore, it can be predicted that the research of water stable MOFs as functional catalysts will experience a boom in the near future. A thorough fundamental investigation on these materials is needed for the understanding of their behaviours under various reaction conditions as well as the nature of their active sites. With that, further exploration on applying MOFs as either participants or solid supports in catalytic activities can be accomplished.

6. Proton Conduction

The unique structural characteristics of MOFs are promising for the development of a new generation proton-conducting materials, which are an important component of electrolyte in batteries and fuel cells. The advantages of applying MOFs for proton conduction include: (1) the inherent crystallinity and structural dynamics allows for smart-design pathway for conductivity; (2) the designable and tunable nature of MOF materials, taking into account the feasible functionalization on both active metal sites and organic ligands, offer great opportunities and infinite possibilities.

There are two distinct types of proton-conducting MOFs have been studied in the current literature: water-mediated and anhydrous,¹⁹⁸ while only the water-mediated cases are relevant in this article. To be suitable for the performance in water-mediated proton-conducting applications, considerable chemical stability under humid conditions is always a prerequisite. The frameworks shall be able to retain a large number of water molecules without inducing irreversible structural decomposition. Therefore, water stable MOFs are the best candidates for water-mediated proton conduction. Some representative cases reported in earlier years (before 2014) have been summarised by Horike *et al.*, Yoon *et al.*, Ramaswamy *et al.* as well as Canivet *et al.*^{14, 78, 79, 199} To avoid overlapping and redundancy, here we emphasise on the recent studies (reported after 2014) on water stable MOFs and their applications in water-mediated proton conduction (Tab. 5). The representative examples are discussed based on the metal valence of water stable MOFs – mono and divalent metal based, and high-valence metal based MOFs.

Table 5. Proton conduction performances of water stable MOFs

Water stable MOF	Conductivity (S cm ⁻¹)	Measurement condition	Ref.
------------------	------------------------------------	-----------------------	------

Na-HPAA	5.6×10^{-3}	24 °C and 98% RH	200
PCMOF10	3.55×10^{-2}	70 °C and 95% RH	201
Ni-MOF-74	2.2×10^{-2}	80 °C and 95% RH	202
Ca-PiPhTA	1.3×10^{-3}	24 °C and 98% RH	203
ZIF-8	4.6×10^{-4}	94 °C and 98% RH	204
(NH ₄) ₂ (adp)[Zn ₂ (ox) ₃ ·3H ₂ O]	8×10^{-3}	25 °C and 100% RH	205
[[Zn(C ₁₀ H ₂ O ₈) _{0.5} (C ₁₀ S ₂ N ₂ H ₈) ₁ ·5H ₂ O] _n]	2.55×10^{-7}	80 °C and 95% RH	57
(((Me ₂ NH ₂) ₃ (SO ₄) ₂ [Zn ₂ (ox) ₃]) _n)	4.2×10^{-2}	25 °C and 98% RH	206
UiO-66(Zr)-(COOH) ₂	2.3×10^{-3}	90 °C and 95% RH	207
UiO-66-(SO ₃ H) ₂	8.4×10^{-2}	80 °C and 90% RH	208
zirconium 2-sulfoterephthalate	5.62×10^{-3}	65 °C and 95% RH	209
[La ₃ L ₄ (H ₂ O) ₆]Cl·xH ₂ O	1.7×10^{-4}	90 °C and 98% RH	210
Tb-DSOA	1.66×10^{-4}	100 °C and 98% RH	34

6.1 Monovalent and divalent metal based water stable MOFs for proton conduction

Bazaga-Garcia *et al.* developed a family of alkali-metal ions with racemic R,S-hydroxyphosphonoacetate, which is termed **M-HPAA** (M = Li, Na, K, Cs).²⁰⁰ All these MOFs possess a high stability under fuel cell working conditions, and provide a proton conductivity in the range 3.5×10^{-5} S cm⁻¹ (Cs-HPAA) to 5.6×10^{-3} S cm⁻¹ (Na-HPAA) at 98% RH and 24 °C. Differences in proton conduction mechanisms, Grothuss (Na⁺ and Cs⁺) or vehicular (Li⁺ and K⁺), are attributed to the different roles played by water molecules and/or proton transfer pathways between phosphonate and carboxylate groups of the ligand HPAA.

Further to monovalent metal based MOFs, a variety of divalent metal based MOFs were developed and applied for proton conduction applications. Ramaswamy *et al.*²⁰¹ reported a layered magnesium carboxyphosphonate framework, **PCMOF10** (Fig. 23), which exhibits an excellent proton conductivity value of 3.55×10^{-2} S cm⁻¹ at 70 °C and 95% RH. PCMOF10 is water stable owing to the strong Mg phosphonate bonds. The 2,5-dicarboxy-1,4-benzenediphosphonic acid ligands deliver a robust backbone and hydrogen phosphonate groups that interact with the lattice water to form an efficient proton transfer pathway.

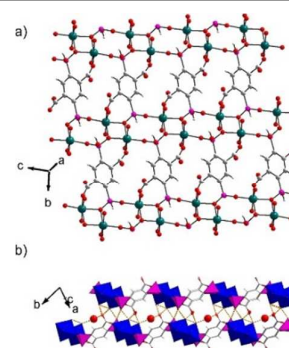


Figure 23. Single crystal structure of PCMOF10: (a) 2-D grid representation. (b) Hydrogen bonding array. (Water molecule: brown).²⁰¹ Reproduced from Ref. 201 with permission, copyright American Chemical Society, 2015.

Also, Dong *et al.* synthesised three new alkaline earth metal based MOFs, namely **M-BPTC** (**M** = **Mg**, **Sr**, **Ba**), using BPTC (2,2',6,6'-tetracarboxybiophenyl) as ligand under hydrothermal conditions.²¹¹ These MOFs exhibit excellent water stability and proton conductivity due to their respective appropriate pathways for proton transport. In addition, as shown in Fig. 24, Phang *et al.* studied **Ni-MOF-74**, $[\text{Ni}_2(\text{dobdc})(\text{H}_2\text{O})_2] \cdot 6\text{H}_2\text{O}$ with hexagonal channels prepared by a microwave-assisted solvothermal reaction.²⁰² The MOF is found to be robust in boiling water for 7 days and in acidic solutions with pH as low as pH 1.8. Soaking Ni-MOF-74 in sulphuric acid solutions at different pH values afforded new proton-conducting frameworks, $\text{H}^+@[\text{Ni}_2(\text{dobdc})]$. At pH 1.8, the acidified MOF shows proton conductivity of $2.2 \times 10^{-2} \text{ S cm}^{-1}$ at 80 °C and 95% RH, comparable to the highest values reported for MOFs. It was found that proton conduction occurs via the Grotthuss mechanism with a significantly low activation energy, and protonated water clusters within the pores of $\text{H}^+@[\text{Ni}_2(\text{dobdc})]$ play an important role in the conduction process.

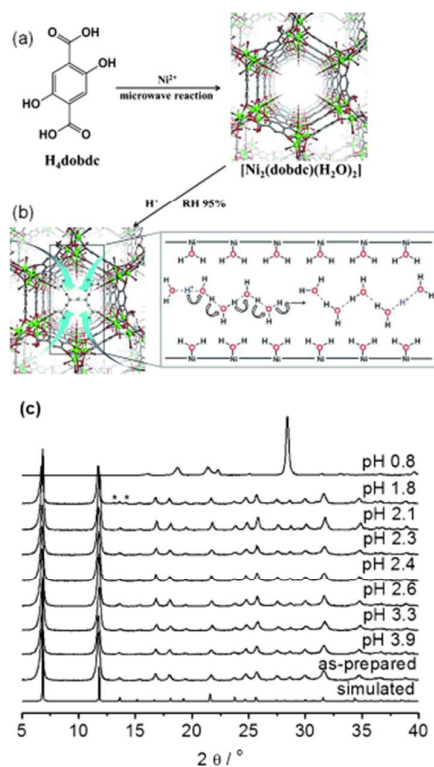


Figure 24. (a) Synthesis and structure of Ni-MOF-74 showing a 1D channel along the c-axis. (b) Cross-sectional view of the pore with protonated water clusters, illustrating a proposed Grotthuss mechanism inside the channel. (c) PXRD data for the simulated, as-prepared, and acidified samples at indicated pH values.²⁰² Reproduced from Ref. 202 with permission, copyright John Wiley and Sons, 2014.

More studies using Ca based MOFs were carried out and applied for proton conduction applications. Typically, Bazaga-

Garcia *et al.* reported that a calcium phosphonate framework,²⁰³ **Ca-PiPhtA**, provides proton conductivity of $5.7 \times 10^{-4} \text{ S cm}^{-1}$ at 98% RH and $T = 24 \text{ }^\circ\text{C}$, which can be further increased to $1.3 \times 10^{-3} \text{ S cm}^{-1}$ upon activation through preheating the sample at 40 °C for 2 h followed by water equilibration at room temperature under controlled conditions.

Besides all these, Zn-based MOFs for proton conduction applications were most extensively analysed.^{57, 204-206, 212} With respect to the classic **ZIF-8**, Barbosa *et al.* examined its proton conductivity.²⁰⁴ The conductivity data of ZIF-8 display strong humidity dependence, increasing by more than 4 orders of magnitude between 20 and 98% RH at 94 °C, ascribed to proton transport along adsorbed water molecules. This is also supported by the enhancement of 1 order of magnitude of the conductivity of samples with highest surface area, attaining a maximum of $4.6 \times 10^{-4} \text{ S cm}^{-1}$ at 94 °C and 98% RH. The value is low, but in agreement with the reported low water uptake capacity of ZIF materials.

Further to ZIF materials, Sadakiyo *et al.* prepared a highly proton-conductive Zn-based MOF, $(\text{NH}_4)_2(\text{adp})[\text{Zn}_2(\text{ox})_3] \cdot 3\text{H}_2\text{O}$ (Fig. 25).²⁰⁵ It was demonstrated that water molecules play a key role in proton conduction as conducting media and serve as triggers to change the proton conductivity through reforming hydrogen-bonding networks by water adsorption/desorption processes. Proton conductivity was consecutively controlled in a wide range from the order of $10^{-12} \text{ S cm}^{-1}$ to $10^{-2} \text{ S cm}^{-1}$ by the humidity. Moreover, Sadakiyo and his co-workers substituted the ammonium ions with potassium ions to form $\text{K}_2(\text{H}_2\text{adp})[\text{Zn}_2(\text{ox})_3] \cdot 3\text{H}_2\text{O}$,²¹³ which has the same crystal structure. By cation substitution in the 2-D layered framework, the highly proton conducting pathway became isomorphous. The result demonstrated that 2-D hydrogen-bonding networks in MOF indeed contribute to the high proton conductivity, and the associated proton conductivity can be deliberately controlled through ion substitution in the well-defined structure of MOF.

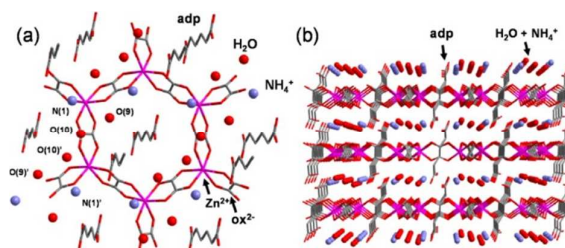


Figure 25. Representation of the crystal structure of $(\text{NH}_4)_2(\text{adp})[\text{Zn}_2(\text{ox})_3] \cdot 3\text{H}_2\text{O}$. (a) Honeycomb layer structure and guest arrangements. (b) Parallel to 2-D layers.²⁰⁵ Reproduced from Ref. 205 with permission, copyright American Chemical Society, 2014.

Moving on, Sanda *et al.* reported the proton conduction properties of a 2D flexible MOF having the molecular formulas $([\text{Zn}(\text{C}_{10}\text{H}_2\text{O}_8)_{0.5}(\text{C}_{10}\text{S}_2\text{N}_2\text{H}_8)] \cdot 5\text{H}_2\text{O})_n$.⁵⁷ It was found that the dimensionality and the internal hydrogen bonding connectivity play a vital role in the resultant conductivity. At high humidity, its conductivity values increase with increasing temperature.

The time-dependent measurements demonstrate its ability to retain conductivity up to 10 h. This MOF could be quite useful for maintaining constant conductivity at elevated temperatures. In addition, Nagarkar *et al.* reported a new 3D MOF, $[(\text{Me}_2\text{NH}_2)_3(\text{SO}_4)_2[\text{Zn}_2(\text{ox})_3]]_n$, that conducts protons under anhydrous as well as humidified conditions.²⁰⁶ The supramolecular net of acid–base pair units provides an efficient proton-conducting pathway under both conditions. Its anhydrous proton conductivity is comparable to that of any MOF-based materials working under similar conditions. The water-assisted proton conductivity is comparable to that of Nafion (currently commercial product), and is the highest proton conductivity among the reported MOF-based materials to date. Especially, unlike other MOFs, which perform only under either humidified or anhydrous conditions, the present compound shows excellent proton conductivity under humidified as well as anhydrous conditions. This renders this MOF as a significant material for further improvements of solid electrolytes and proton conductors.

6.2 High-valence metal based water stable MOFs for proton conduction

Several researchers have looked into the ionic conductivity of water stable **UiO-66 and its functionalized analogues**.^{207, 208, 214, 215} Borges *et al.*²⁰⁷ reported that UiO-66(Zr)-(COOH)₂ provides a superior proton conductivity of $2.3 \times 10^{-3} \text{ S cm}^{-1}$ at 90 °C and 95% RH, which also combines with a good water stability and a low cost and environmental friendly synthesis. Furthermore, Phang *et al.*²⁰⁸ used UiO-66-(SO₃H)₂ that exhibited an even better proton conductivity of $8.4 \times 10^{-2} \text{ S cm}^{-1}$ at 80 °C and 90% RH, as shown in Fig. 26. A long-term stability of the conductivity was also observed. Also, Planchais *et al.*²¹⁵ identified that the proton conduction capability of UiO-66 based materials at room temperature increases with the water uptake as well as the concentration of the free acidic carboxylic functions. It was revealed that water molecules preferentially form interconnected clusters within the UiO-66 cages and generate a hydrogen-bonding network responsible for the proton propagation, and also water molecules could strongly interact with the –COOH grafted functions, resulting in the additional charge carriers.

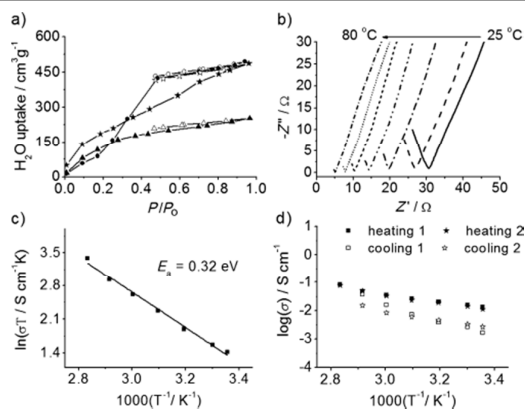


Figure 26. (a) Water-vapour-adsorption/desorption isotherms of UiO-66 (circles), UiO-66(SH)₂ (triangles), and UiO-66(SO₃H)₂ (stars) at 25 °C. Filled and open symbols indicate adsorption and desorption, respectively. (b) Impedance spectra, (c) Arrhenius plot, and (d) log-scaled proton conductivities for UiO-66(SO₃H)₂ at 90% RH.²⁰⁸ Reproduced from Ref. 208 with permission, copyright John Wiley and Sons, 2015.

Further to UiO-66 materials, Taylor *et al.* reported a new and unique structure of a **zirconium 2-sulfoterephthalate** MOF, containing an ordered defect sublattice.²⁰⁹ It was found that defect control could considerably enhance the proton conductivity in addition to conventional method of increasing overall acidity. This highly porous MOF was lined with sulfonic acid groups, implying a high proton concentration in the pore. This acid treatment was to saturate the charge trapping sites and improve the overall conductivity. As a result, by synthesis in the presence of sulfoacetic acid, a 5-fold improvement of the conductivity was achieved, reaching a maximum of $5.62 \times 10^{-3} \text{ S cm}^{-1}$ at 95% RH and 65 °C.

Besides Zr-based MOFs, lanthanide metal-based MOFs were also studied for proton conduction applications. Begum *et al.* synthesised a new 3D triazolyl-phosphonate-based La³⁺ MOF, $[\text{La}_3\text{L}_4(\text{H}_2\text{O})_6]\text{Cl} \cdot x\text{H}_2\text{O}$, with large hydrophilic channels (1.9 nm) containing water molecules as proton-conducting medium.²¹⁰ The MOF forms a water-stable, porous structure that can be reversibly hydrated and dehydrated. This MOF material accomplishes the challenges of water stability and proton conduction even at 110 °C, while the conductivity is proposed to occur by the vehicle mechanism. It was also found that the proton conductivity increases significantly with increasing temperature and RH by facilitating charge formation and maintaining high charge density, respectively. Moreover, Dong *et al.* developed a new 3D porous terbium-MOF, $[\text{Tb}_4(\text{OH})_4(\text{DSOA})_2(\text{H}_2\text{O})_8] \cdot (\text{H}_2\text{O})_8$ (Tb-DSOA), using Tb³⁺ ions and a sulfonate–carboxylate linker disodium-2,2'-disulfonate-4,4'-oxydibenzoic acid (Na₂H₂DSOA).³⁴ It features a porous luminescent robust framework and 1D open hydrophilic channels decorated by uncoordinated sulfonate oxygen atoms and aqua ligands. Exceptional water-stability makes this MOF compatible for applications in aqueous solution. In particular, the noncoordinated sulfonate oxygen atoms functionalize its channels could act as hopping sites for proton transfer, resulting in a proton conductivity of $1.66 \times 10^{-4} \text{ S cm}^{-1}$ at 98% RH.

6.3 Perspectives

Researchers in this field of proton conductive MOFs have made a considerable achievement in the past several years, as initially most MOFs are electron insulators and do not provide any efficient pathway or carrier for proton transport. Now, a variety of 2D and 3D water stable MOFs with high proton mobility and conductivity at low temperatures have been developed; some in this class of materials can even compete with the commercial available product – Nafion. Tactical strategies (e.g. hydrogen bonding networks) that give rise to excellent proton conduction have been analysed and introduced to the well-defined crystal structures of water stable MOF materials.

Despite the significant advances in absolute conductivity and robustness of conductive MOFs, there are still critical challenges remaining for the further development of MOF proton conductors. Significant future work is required before the nature of proton conduction in MOFs can be fully understood. Besides gaining more sophisticated fundamental understanding, scientists shall work on developing better MOF materials with novel topologies and active metal-ligand networks, as well as the molding technologies to address the brittleness and compatibility for incorporation into the electrochemical devices.

At the same time, there are plenty of opportunities for the purpose of academic research and commercial development. Typically, the crystalline nature of MOFs provide distinctive chances to study the mechanism of proton conduction on a molecular/atomic level. Moreover, the designable and tunable natures of MOFs would allow for the continuing development with respect to the synthetic and applied works in this field. In the coming future, we believe that water stable MOFs have a great potential to become one of the most important class of materials in electrochemical industries, embracing great proton conductivity and precisely controlled functionality.

7. Conclusions

MOF as a new class of porous materials has been a much-discussed topic over the last decade. The prototypical MOFs developed in earlier years have attracted tremendous attention because of their outstanding specific surfaces as well as calibrated pore sizes. Researchers managed to apply these pioneering porous materials in fields like gas storage and separation. However, the water stability of these MOFs was a huge problem as the materials tend to undergo irreversible structural degradation in a water-containing environment. As a result, pre-treatment to exclude water must be introduced in respective applications, which acted as the chief limitation for MOF materials to be widely applied in practice. Hence, the development of water stable MOFs becomes necessary, to cope with the vast and complex water effects on diverse applications.

With the constant efforts to disclose the relationship between MOF structure and hydro-stability and study the strategies for water stable MOFs synthesis, nowadays, more and more water stable MOFs are evolved. On a very high level, they can be grouped into three categories: metal carboxylate frameworks consisting of high-valence metal ions, metal azolate frameworks, and MOFs with special functionalization. Along with the more consolidated database of water stable MOFs, visionary researchers have been exploring the feasibility of MOFs in a range of water-related applications. In this review, significant studies of using water stable MOFs for adsorption, membrane separation, sensing, catalysis and proton conduction were comprehensively discussed. Promising performance has been observed owing to the undeniable advantages of MOF-type materials, such as huge porosity, easy tunability of their pore size, and multiple shapes from micro- to meso-porous scale through modifying the connectivity of

inorganic moieties and the nature of organic linkers. As far as we are concerned, significant work has been achieved applying water stable MOF materials as adsorbents and sensors; while there is still a large room for development in MOF-based membranes, catalysts and proton conductors studies.

Overall, this review provides a comprehensive picture of water stable MOF applications and significant insights of the respective materials and processes. Taking a step further to the applications, surveying water stability research of MOFs over the past decade, it experiences several milestones: from water sensitive to relatively moisture stable, then to water stable and now ultra-stable MOFs. The quest of high-demand water stable MOFs, while keeping their favourable properties, would never stop. Researchers continue to search for revolutionary MOF structures, and future research should target on the development of functional MOFs that not only stay stable in water, but also can maintain its robustness in real industrial conditions. The water stable MOFs with better performance would have a great potential to triumph over the conventional porous materials currently applied in various industrial sectors.

Acknowledgements

This work was supported by the research funding provided by Engineering and Physical Sciences Research Council in the United Kingdom (Grant no. EPSRC, EP/J014974/1). The authors gratefully acknowledge Dr. Melanie Lee for her precious time and contribution in fine-tuning the manuscript. C. Wang acknowledges the National University of Singapore Graduate School for Integrative Sciences and Engineering scholarship.

Appendix

Molecular structural information and ligand abbreviations of mentioned MOFs

MOF	Molecular formula	Ligand information
AEMOF-1	[Mg(H ₂ dhtp)(H ₂ O) ₂]-DMAc	H ₂ dhtp=2,5-dihydroxy-terephthalic acid; DMAc=N,N-dimethylacetamide.
Al ₂ (OH) ₂ TCPP-Co	Al ₂ (OH) ₂ TCPP-Co	TCPP = 4,4',4'',4'''-(porphyrin-5,10,15,20-tetrayl)tetrabenzoate
BFMOF-1	Pb ₆ O ₂ (C ₆₉ H ₄₈ O ₁₂ S ₄) ₂ (DMA) ₃ (H ₂ O) ₂	DMA = N,N-dimethylacetamide
bio-MOF-1	Zn ₈ (ad) ₄ (BPDC) ₆ O-2Me ₂ NH ₂	ad = adeninate; BPDC = biphenyl dicarboxylic acid.
Ca-PiPhtA	Ca ₂ [(HO ₃ PC ₆ H ₃ COOH) ₂] ₂ [(H ₂ O ₃ PC ₆ H ₃ (COO) ₂ H)(H ₂ O) ₂]-5H ₂ O	PiPhtA = 5-(dihydroxyphosphoryl)isophthalic acid
CALF-25	BaH ₂ L	Barium tetraethyl-1,3,6,8-pyrenetetraphosphonate
CAU-1	[Al ₄ (OH) ₂ (OCH ₃) ₄ (H ₂ N-bdc) ₃]-x H ₂ O	bdc = 1,4-benzenedicarboxylate (terephthalate)
CAU-10	[Al(OH)(m-BDC-X) _{1-y} (m-BDC-SO ₃ H) _y](X=H, NO ₂ , OH)	H ₂ BDC=1,3-benzenedicarboxylic acid
Cd-EDDA	[(Cd _{1.5} (C ₁₈ H ₁₀ O ₁₀)] _n -(H ₃ O)(H ₂ O) ₃] _n	-
[Cd ₂ L ₂]-NMP-M	[Cd ₂ L ₂]-NMP-MeOH	H ₂ L = 2-(3,5-dimethyl-1H-

Journal Name

ARTICLE

eOH		pyrazol-4-yl)-1,3-dioxoisindoline-5,6-dicarboxylic acid; NMP = 1-methyl-2-pyrrolidinone.	MAF-7	Zn(mtz) ₂	mtz = 3-methyl-1,2,4-triazolate
[Cd ₂ (TBA) ₂ (bipy)(DMA) ₂]	[Cd ₂ (TBA) ₂ (bipy)(DMA) ₂]	H ₂ TBA = 4-(1H-tetrazol-5-yl)-benzoic acid; bipy = 4,4'-bipyridine.	MAF-49	Zn(batz)	H ₂ batz = Bis(5-amino-1H-1,2,4-triazol-3-yl)methane
[(C ₂ H ₅) ₂ NH ₂] ₂ [Mn ₆ (L)(OH) ₂ (H ₂ O) ₆]-4DEF	[(C ₂ H ₅) ₂ NH ₂] ₂ [Mn ₆ (L)(OH) ₂ (H ₂ O) ₆]-4DEF	H ₁₂ L = 5,5',5'',5''',5''''- [1,2,3,4,5,6-phenylhexamethoxy] hexaisophthalic acid; DEF = N,N'-diethylformamide.	MAF-X25ox	[Mn ^{II} Mn ^{III} (OH)Cl ₂ (bbta)]	H ₂ bbta = 1H,5H-benzo(1,2-d:4,5-d')bistriazole ox = oxalate.
Co/Zn-BTTBBPY	Co ₂ (BTTB)-(BPY)	BTTB = 4,4',4'',4'''-benzene-1,2,4,5-tetrahydropyridine; BPY = bipyridine.	Mg-CUK-1 MIL-53(Cr) MIL-68	[Mg ₃ (2,4-pdc) ₂ (OH) ₂] Cr(OH)(BDC) Fe(OH)(bdc)	pdc = pyridinedicarboxylate BDC = (O ₂ C)-C ₆ H ₄ -(CO ₂) bdc = 1,4-benzenedicarboxylate (terephthalate)
[Co ₄ L ₃ (μ ₃ -OH)(H ₂ O) ₃](SO ₄) _{0.5}	[Co ₄ L ₃ (μ ₃ -OH)(H ₂ O) ₃](SO ₄) _{0.5}	L = 4-(4H-1,2,4-triazol-4-yl)-phenyl phosphonate	MIL-96	Al ₁₂ O(OH) ₁₈ (H ₂ O) ₃ (Al ₂ (OH) ₄)(BTC) ₆ ·24H ₂ O	BTC=1,3,5-benzenetricarboxylate
Co-ZIF-9	Co(bl _m)	bl _m = benzimidazole	MIL-100	Fe ₃ O(C ₆ H ₃ (CO ₂) ₃) ₂	-
CPM-17-Zn	Ca[Zn ₂ (p-murea) ₆] ₄ [In ₃ (BTC) ₆] ₂	p-murea = 1,3-dimethylpropyleneurea; BTC=1,3,5-benzenetricarboxylate.	MIL-101 MIL-121	Cr ₃ F(H ₂ O) ₂ O(BDC) ₃ Al(OH)[H ₂ btec]-(guest) (guest = H ₂ O, H ₄ btec)	BDC = (O ₂ C)-C ₆ H ₄ -(CO ₂) H ₂ btec = 1,2,4,5-benzenetetracarboxylic acid, pyromellitic acid
Cu-bipy-BTC	Cu-bipy-BTC	bipy = 2,2'-bipyridine; BTC = 1,3,5-tricarboxylate.	MIL-124	Ga ₂ (OH) ₄ (C ₉ O ₆ H ₄)	-
Cu(I)-MOF	CH ₃ CN·MeOH·1.5H ₂ O·Cu ₂ (L) ₂	L = 1-benzimidazolyl-3,5-bis(4-pyridyl)benzene	MIL-160	AlO ₆ C ₆ H ₃	FDCA = 2,5-furandicarboxylic acid
Cu ₂ L	Cu ₂ L	L=3,3',5,5'-tetraethyl-4,4'-bipyrazolate	MIL-163	Zr(H ₂ -TzGal)	H ₆ -TzGal = 5,5'-(1,2,4,5-tetrazine-3,6-diyl)bis(benzene-1,2,3-triol)
Cu ₆ (trz) ₁₀ (H ₂ O) ₄ [H ₂ SiW ₁₂ O ₄₀]-8H ₂ O	Cu ₆ (trz) ₁₀ (H ₂ O) ₄ [H ₂ SiW ₁₂ O ₄₀]-8H ₂ O	trz = 1,2,4-triazole	mmen-Mg ₂ (dobpdc)	mmen-Mg ₂ (dobpdc)	mmen = N,N'-dimethylethylenediamine; dobpdc = 4,4'-dioxidobiphenyl-3,3'-dicarboxylate
[(Dy(Cmdcp)(H ₂ O) ₃)(NO ₃)-2H ₂ O] _n	[(Dy(Cmdcp)(H ₂ O) ₃)(NO ₃)-2H ₂ O] _n	Cmdcp = N-carboxymethyl-(3,5-dicarboxyl)pyridine	MOF-5 MOF-74	Zn ₄ O(BDC) ₃ [Mg ₂ (dobdc)(H ₂ O) ₂]-6H ₂ O	BDC = (O ₂ C)-C ₆ H ₄ -(CO ₂) dobdc = 2,5-dioxido-1,4-benzenedicarboxylate
[Eu ₃ (bpydb) ₃ (HCOO)(OH) ₂ (DMF)]·(DMF) ₃ (H ₂ O) ₂	[Eu ₃ (bpydb) ₃ (HCOO)(OH) ₂ (DMF)]·(DMF) ₃ (H ₂ O) ₂	bpydbH ₂ = 4,4'-(4,4'-bipyridine-2,6-diyl) dibenzoic acid; DMF = dimethylformamide.	MOF-801 MOF-808	Zr ₆ O ₄ (OH) ₄ (fumarate) ₆ Zr ₆ O ₄ (OH) ₄ -(BTC) ₂ (HCOO) ₅ (H ₂ O) ₂	BTC = 1,3,5-benzenetricarboxylate
[Eu(HL)(H ₂ O) ₂] _n ·2H ₂ O	[Eu(HL)(H ₂ O) ₂] _n ·2H ₂ O	L = 3,5-di(2,4-dicarboxylphenyl)pyridine	MOF-841	Zr ₆ O ₄ (OH) ₄ (MTB) ₂ (HCOO) ₄ (H ₂ O) ₄	H ₄ MTB = 4,4',4'',4'''-Methanetetrayltetrazobenzoic acid
FIR-54	[Zn(Tipa)]·2NO ₃ ·DMF·4H ₂ O	Tipa = tris(4-(1H-imidazol-1-yl)phenyl)amine; DMF = dimethylformamide.	Na-HPAA	Na ₂ (OOCCH(OH)PO ₃ H)(H ₂ O) ₄	HPAA = hydroxyphosphonoacetate
FJI-H6	[Zr ₆ O ₄ (OH) ₄ (H ₂ TBPP) ₃] _n	H ₆ TBPP = 4',4'',4''',4''''-(porphyrin-5,10,15,20-tetrayl)tetrakis([1,1'-biphenyl]-4-carboxylic acid)	NENU-1 NENU-500	[Cu ₂ (BTC) _{4/3} (H ₂ O) ₂] ₆ [H ₂ SiW ₁₂ O ₄₀](C ₄ H ₁₂ N) ₂ [TBA] ₃ [PMO ^V ₈ Mo ^{VI} ₄ O ₃₆ (OH) ₄ Zn ₄][BTB] _{4/3}	BTC = 1,3,5-benzenetricarboxylate BTB = benzene tribenzoate; TBA = tetrabutylammonium ion
FMOF-1	Ag ₄ Tz ₆	Tz = 3,5-bis(trifluoromethyl)-1,2,4-triazolate	NH ₂ -MIL-125 (NH ₄) ₂ (adp)[Zn ₂ (ox) ₃]-3H ₂ O [Ni(BPEB)]	Ti ₈ O ₈ (OH) ₄ (C ₆ H ₃ C ₂ O ₄ NH ₂) ₆ (NH ₄) ₂ (adp)[Zn ₂ (ox) ₃]-3H ₂ O	-
HKUST-1	Cu ₃ (BTC) ₂ (H ₂ O) ₃	BTC=1,3,5-benzenetricarboxylate	NU-1000 NU-1100	Zr ₆ (OH) ₈ (OH) ₈ (TBAPy) ₂ Zr ₆ (OH) ₄ (OH) ₄ (L) ₄	adp = adipic acid; ox = oxalate.
InPCF-1	(H ₃ O)[In(pbpdcc)]·3H ₂ O	pbpdcc=4'-phosphonobiphenyl-3,5-dicarboxylate	IRMOF-74-III	Mg ₂ (DH3PhDC)	H ₂ BPEB = 1,4-bis(1H-pyrazol-4-ylethynyl)benzene TBAPy = 1,3,6,8-tetrakis(p-benzoic acid)pyrene
IRMOF-74-III	Mg ₂ (DH3PhDC)	H ₄ DH3PhDC = 2',5'-dimethyl-3,3''-dihydroxy-[1,1':4',1''-terphenyl]-4,4''-dicarboxylic acid	NU-1105	C ₃₁₂ H ₂₁₀ O ₃₂ Zr ₆	L ₄ H = 4-[2-[3,6,8-tris(2-(4-carboxyphenyl)-ethynyl)-pyren-1-yl]ethynyl]-benzoic acid
JLU-Liu18	[NO ₃][In ₃ OL ₃]-4DMF·3H ₂ O	L = pyridine-3,5-bis(phenyl-4-carboxylate); DMF = dimethylformamide.	PCMOF10	Mg ₂ (H ₂ O) ₄ (H ₂ L)·H ₂ O	(Zr ₆ -oxo clusters) (ligand = Py-FF)
[La ₃ L ₄ (H ₂ O) ₆]Cl·xH ₂ O	[La ₃ L ₄ (H ₂ O) ₆]Cl·xH ₂ O	L = 4-(4H-1,2,4-triazol-4-yl)phenyl phosphonate.	PCN-222	C ₄₈ H ₃₂ ClFeN ₄ O ₁₆ Zr ₃	H ₆ L = 2,5-dicarboxy-1,4-benzene-diphosphonic acid
[La(py ₂ zdc) _{1.5} (H ₂ O) ₂]-2H ₂ O	[La(py ₂ zdc) _{1.5} (H ₂ O) ₂]-2H ₂ O	py ₂ zdc = 2,3-pyrazinedicarboxylate	PCN-228	Zr ₆ (OH) ₄ O ₄ (TCP-1) ₃ ·10DMF·2H ₂ O	Fe-TCPP (TCPP=tetrakis(4-carboxyphenyl)porphyrin)
M ₃ (BTP) ₂ (M = Ni, Cu, Zn, Co)	Ni ₃ (BTP) ₂ ·3CH ₃ OH·10H ₂ O	H ₃ BTP = 1,3,5-tris(1H-pyrazol-4-yl)benzene	PCN-229	Zr ₆ (OH) ₄ O ₄ (TCP-2) ₃ ·45DMF·25H ₂ O	TCP = tetrakis(4-carboxyphenyl)porphyrin;
MAF-6	Zn(eim) ₂	eim = 2-ethylimidazole			DMF = dimethylformamide.

ARTICLE

Journal Name

PCN-230	$Zr_6(OH)_4(O_4(TCP-3))_3 \cdot 30DMF \cdot 10H_2O$	DMF = dimethylformamide. TCP = tetrakis(4-carboxyphenyl)porphyrin; DMF = dimethylformamide.
PCN-521	$[Zr_6(OH)_8(OH)_8]L_2$	L = 4',4'',4''',4''''-methanetetrayltetrabiphenyl-4-carboxylate, MTBC
PCN-523	$[Hf_6(OH)_8(OH)_8]L_2$	L = MTBC
PCN-601	$[Ni_8(OH)_4(H_2O)_2Pz_{12}]TPP$	Pz = pyrazolate; $H_4TPP = 5,10,15,20$ -tetra(1H-pyrazol-4-yl)porphyrin.
PCN-777	$Zr_6(O)_4(OH)_{10}(H_2O)_6(TATB)_2$	TATB = 4,4',4''-s-triazine-2,4,6-triyl-tribenzoate
PCP-33	$(Cu_4Cl)(BTBA)_8 \cdot (CH_3)_2NH_2 \cdot (H_2O)_{12}$	H3BTBA = 3,5-bis(2H-tetrazol-5-yl)-benzoic acid
Tb-DSOA	$([Tb_4(OH)_4(DSOA)_2(H_2O)_8] \cdot (H_2O)_8)_n$	DSOA = 2,2'-disulfonate-4,4'-oxydibenzoic acid
$([Tb(L)_{1.5}(H_2O)] \cdot 3H_2O)_n$	$([Tb(L)_{1.5}(H_2O)] \cdot 3H_2O)_n$	$L_1 = 2$ -(2-Hydroxypropionylamino)-terephthalate
$[Tb(L)(OH)] \cdot x(solv)$	$[Tb(L)(OH)] \cdot x(solv)$	$L = 5$ -(4-carboxyphenyl)pyridine-2-carboxylate
UiO-66	$Zr_6O_4(OH)_4(BDC)_6$	BDC = (O ₂ C)-C ₆ H ₄ -(CO ₂)
UiO-67	$Zr_6O_4(OH)_4(bpdc)_6$	bpdc = biphenyldicarboxylate, O ₂ C(C ₆ H ₄) ₂ CO ₂
UiO-68	$Zr_6O_4(OH)_4(C_{20}H_{10}O_4)_6$	-
ZIF-7	Zn(bim) ₂	Hbim = benzimidazole
ZIF-8	Zn(mim) ₂	Hmim = 2-methylimidazole
ZIF-67	Co(mim) ₂	Hmim = 2-methylimidazole
ZIF-90	Zn(C ₄ H ₃ N ₂ O) ₂	2-carboxaldehyde imidazole
Zn ₃ (btc) ₂ · 12H ₂ O	Zn ₃ (btc) ₂ · 12H ₂ O	btc = 1,3,5-benzenetricarboxylate
$([Zn(C_{10}H_2O_8)_{0.5}(C_{10}S_2N_2H_8)] \cdot 5H_2O)_n$	$([Zn(C_{10}H_2O_8)_{0.5}(C_{10}S_2N_2H_8)] \cdot 5H_2O)_n$	-
$[Zn_4(Hbvpv)_2(BTC)_3(HCOO)(H_2O)_2] \cdot 4H_2O$	$[Zn_4(Hbvpv)_2(BTC)_3(HCOO)(H_2O)_2] \cdot 4H_2O$	hbvpv = 3,5-bis-(2-(pyridin-4-yl)vinyl)pyridine; BTC = 1,3,5-tricarboxylate.
Zn(IM) _{1.5} (abIM) _{0.5}	Zn(IM) _{1.5} (abIM) _{0.5}	IM = imidazole; abIM = 2-aminobenzimidazole.
Zn ₄ (μ ₄ -O)-(μ ₄ -4-carboxy-3,5-dimethyl-4-carboxy-pyrazolato) ₃	Zn ₄ (O)-(4-carboxy-3,5-dimethyl-4-carboxy-pyrazolato) ₃	-
Zn-pbdc	Zn-pbdc	pbdc = poly(1,4-benzenedicarboxylate)
Zn ₂ TCS(4,4'-bipy)	Zn ₂ TCS(4,4'-bipy)	TCS = tetrakis(4-carboxyphenyl)silane; bipy = bipyridine.
$[Zn(trz)(H_2betc)_{0.5}] \cdot DMF$	$[Zn(trz)(H_2betc)_{0.5}] \cdot DMF$	trz = 1,2,4-triazole; $H_4betc =$ pyromellitic acid; DMF = dimethylformamide.
$[Zn_{12}(trz)_{20}][SiW_{12}O_{40}] \cdot 11H_2O$	$[Zn_{12}(trz)_{20}][SiW_{12}O_{40}] \cdot 11H_2O$	trz = 1,2,4-triazole; SiW ₁₂ O ₄₀ : Keggin-type anion.
$[Zr_6O_4(OH)_4(btba)_3](DMF)_x(H_2O)_y$	$[Zr_6O_4(OH)_4(btba)_3](DMF)_x(H_2O)_y$	btba = N,N'-bis(trimethylsilyl)benzamide; DMF = dimethylformamide.

Note: AEMOF – alkaline earth metal-organic framework; BFMOF – backfolded metal-organic framework; CALF – Calgary Framework; CAU – Christian Albrechts University; CPP – coordination polymer particle; FIR/FJI – Fujian Institute of Research; HKUST – Hong Kong University of Science and Technology; IRMOF – isoreticular metal-organic framework; JLU – Jilin University; MAF – metal azolate framework; CUK – Cambridge University-KRICT; MIL – Matériel Institut Lavoisier; NENU – Northeast Normal University; NU – Northwestern University; PCP – Porous Coordination Polymer; PCMOF – proton-conducting metal-organic framework; PCN – porous coordination network; UiO – University of Oslo; ZIF – Zeolitic Imidazolate Framework.

Notes and references

- H. C. Zhou, J. R. Long and O. M. Yaghi, *Chemical Reviews*, 2012, **112**, 673.
- H. C. Zhou and S. Kitagawa, *Chemical Society Reviews*, 2014, **43**, 5415.
- H. Furukawa, K. E. Cordova, M. O'Keeffe and O. M. Yaghi, *Science*, 2013, **341**, 1230444.
- M. Li, D. Li, M. O'Keeffe and O. M. Yaghi, *Chemical Reviews*, 2014, **114**, 1343.
- S. M. Cohen, *Chemical Reviews*, 2012, **112**, 970.
- J. D. Evans, C. J. Sumbry and C. J. Doonan, *Chemical Society Reviews*, 2014, **43**, 5933.
- P. Deria, J. E. Mondloch, O. Karagiari, W. Bury, J. T. Hupp and O. K. Farha, *Chemical Society Reviews*, 2014, **43**, 5896.
- Y.-B. Zhang, H. Furukawa, N. Ko, W. Nie, H. J. Park, S. Okajima, K. E. Cordova, H. Deng, J. Kim and O. M. Yaghi, *Journal of the American Chemical Society*, 2015, **137**, 2641.
- L. Huang, H. Wang, J. Chen, Z. Wang, J. Sun, D. Zhao and Y. Yan, *Microporous and Mesoporous Materials*, 2003, **58**, 105.
- P. M. Schoencker, C. G. Carson, H. Jasuja, C. J. J. Flemming and K. S. Walton, *Industrial & Engineering Chemistry Research*, 2012, **51**, 6513.
- H. Li, M. Eddaoudi, M. O'Keeffe and O. M. Yaghi, *Nature*, 1999, **402**, 276.
- S. S. Kaye, A. Dailly, O. M. Yaghi and J. R. Long, *Journal of the American Chemical Society*, 2007, **129**, 14176.
- N. C. Burtch, H. Jasuja and K. S. Walton, *Chemical Reviews*, 2014, **114**, 10575.
- J. Canivet, A. Fateeva, Y. Guo, B. Coasne and D. Farrusseng, *Chemical Society Reviews*, 2014, **43**, 5594.
- A. J. Howarth, Y. Liu, P. Li, Z. Li, T. C. Wang, J. T. Hupp and O. K. Farha, *Nature Reviews Materials*, 2016, **1**, 15018.
- M. Bosch, M. Zhang and H.-C. Zhou, *Advances in Chemistry*, 2014, **2014**, 1.
- N. u. Qadir, S. A. M. Said and H. M. Bahaidarah, *Microporous and Mesoporous Materials*, 2015, **201**, 61.
- G. Ferey, C. Mellot-Draznieks, C. Serre, F. Millange, J. Dutour, S. Surble and I. Margiolaki, *Science*, 2005, **309**, 2040.
- J. H. Cavka, S. Jakobsen, U. Olsbye, N. Guillou, C. Lamberti, S. Bordiga and K. P. Lillerud, *Journal of the American Chemical Society*, 2008, **130**, 13850.
- Y. Bai, Y. Dou, L. H. Xie, W. Rutledge, J. R. Li and H. C. Zhou, *Chemical Society Reviews*, 2016, **45**, 2327.
- T.-F. Liu, D. Feng, Y.-P. Chen, L. Zou, M. Bosch, S. Yuan, Z. Wei, S. Fordham, K. Wang and H.-C. Zhou, *Journal of the American Chemical Society*, 2015, **137**, 413.
- M. Zhang, Y.-P. Chen, M. Bosch, T. Gentle, K. Wang, D. Feng, Z. U. Wang and H.-C. Zhou, *Angewandte Chemie International Edition*, 2014, **53**, 815.
- D. Feng, K. Wang, J. Su, T.-F. Liu, J. Park, Z. Wei, M. Bosch, A. Yakovenko, X. Zou and H.-C. Zhou, *Angewandte Chemie International Edition*, 2015, **54**, 149.
- P. Deria, Y. G. Chung, R. Q. Snurr, J. T. Hupp and O. K. Farha, *Chemical Science*, 2015, **6**, 5172.
- P. Deria, D. A. Gomez-Gualdrón, W. Bury, H. T. Schaeff, T. C. Wang, P. K. Thallapally, A. A. Sarjeant, R. Q. Snurr, J. T. Hupp and O. K. Farha, *Journal of the American Chemical Society*, 2015, **137**, 13183.
- S.-Y. Moon, Y. Liu, J. T. Hupp and O. K. Farha, *Angewandte Chemie International Edition*, 2015, **54**, 6795.
- A. Cadiau, J. S. Lee, D. Damasceno Borges, P. Fabry, T. Devic, M. T. Wharmby, C. Martineau, D. Foucher, F. Taulelle, C.-H. Jun, Y. K. Hwang, N. Stock, M. F. De Lange, F. Kapteijn, J. Gascon, G. Maurin, J.-S. Chang and C. Serre, *Advanced Materials*, 2015, **27**, 4775.
- G. Mouchaham, L. Cooper, N. Guillou, C. Martineau, E. Elkaïm, S. Bourrelly, P. L. Llewellyn, C. Allain, G. Clavier, C. Serre and T. Devic, *Angewandte Chemie International Edition*, 2015, **54**, 13297.
- J. Zheng, M. Wu, F. Jiang, W. Su and M. Hong, *Chemical Science*, 2015, **6**, 3466.

30. S. B. Kalidindi, S. Nayak, M. E. Briggs, S. Jansat, A. P. Katsoulidis, G. J. Miller, J. E. Warren, D. Antypov, F. Cora, B. Slater, M. R. Prestly, C. Marti-Gastaldo and M. J. Rosseinsky, *Angewandte Chemie-International Edition*, 2015, **54**, 221.
31. R. Plessius, R. Kromhout, A. L. Ramos, M. Ferbinteanu, M. C. Mittelmeijer-Hazeleger, R. Krishna, G. Rothenberg and S. Tanase, *Chemistry*, 2014, **20**, 7922.
32. L. Qin, L.-X. Lin, Z.-P. Fang, S.-P. Yang, G.-H. Qiu, J.-X. Chen and W.-H. Chen, *Chemical Communications*, 2016, **52**, 132.
33. Y.-T. Liang, G.-P. Yang, B. Liu, Y.-T. Yan, Z.-P. Xi and Y.-Y. Wang, *Dalton Transactions*, 2015, **44**, 13325.
34. X.-Y. Dong, R. Wang, J.-Z. Wang, S.-Q. Zang and T. C. W. Mak, *Journal of Materials Chemistry A*, 2015, **3**, 641.
35. J. Qin, B. Ma, X.-F. Liu, H.-L. Lu, X.-Y. Dong, S.-Q. Zang and H. Hou, *Journal of Materials Chemistry A*, 2015, **3**, 12690.
36. L.-H. Cao, F. Shi, W.-M. Zhang, S.-Q. Zang and T. C. W. Mak, *Chemistry-a European Journal*, 2015, **21**, 15705.
37. S. Yao, D. Wang, Y. Cao, G. Li, Q. Huo and Y. Liu, *Journal of Materials Chemistry A*, 2015, **3**, 16627.
38. W. Dan, X. Liu, M. Deng, Y. Ling, Z. Chen and Y. Zhou, *Dalton Transactions*, 2015, **44**, 3794.
39. J.-N. Hao and B. Yan, *Chemical Communications*, 2015, **51**, 14509.
40. N. Reimer, B. Bueken, S. Leubner, C. Seidler, M. Wark, D. De Vos and N. Stock, *Chemistry*, 2015, **21**, 12517.
41. J. P. Zhang, Y. B. Zhang, J. B. Lin and X. M. Chen, *Chemical Reviews*, 2012, **112**, 1001.
42. R. Banerjee, A. Phan, B. Wang, C. Knobler, H. Furukawa, M. O'Keeffe and O. M. Yaghi, *Science*, 2008, **319**, 939.
43. K. S. Park, Z. Ni, A. P. Cote, J. Y. Choi, R. Huang, F. J. Uribe-Romo, H. K. Chae, M. O'Keeffe and O. M. Yaghi, *Proceedings of the National Academy of Sciences*, 2006, **103**, 10186.
44. X.-C. Huang, Y.-Y. Lin, J.-P. Zhang and X.-M. Chen, *Angewandte Chemie International Edition*, 2006, **45**, 1557.
45. V. Colombo, S. Galli, H. J. Choi, G. D. Han, A. Maspero, G. Palmisano, N. Masciocchi and J. R. Long, *Chemical Science*, 2011, **2**, 1311.
46. J. P. Zhang, A. X. Zhu, R. B. Lin, X. L. Qi and X. M. Chen, *Advanced Materials*, 2011, **23**, 1268.
47. P. Q. Liao, D. D. Zhou, A. X. Zhu, L. Jiang, R. B. Lin, J. P. Zhang and X. M. Chen, *Journal of the American Chemical Society*, 2012, **134**, 17380.
48. C.-T. He, J.-Y. Tian, S.-Y. Liu, G. Ouyang, J.-P. Zhang and X.-M. Chen, *Chemical Science*, 2013, **4**, 351.
49. P. Q. Liao, W. X. Zhang, J. P. Zhang and X. M. Chen, *Nature Communications*, 2015, **6**, 8697.
50. C. T. He, L. Jiang, Z. M. Ye, R. Krishna, Z. S. Zhong, P. Q. Liao, J. Xu, G. Ouyang, J. P. Zhang and X. M. Chen, *Journal of the American Chemical Society*, 2015, **137**, 7217.
51. H.-R. Fu, Z.-X. Xu and J. Zhang, *Chemistry of Materials*, 2015, **27**, 205.
52. E.-L. Zhou, C. Qin, X.-L. Wang, K.-Z. Shao and Z.-M. Su, *Chemistry-a European Journal*, 2015, **21**, 13058.
53. X. Meng, R.-L. Zhong, X.-Z. Song, S.-Y. Song, Z.-M. Hao, M. Zhu, S.-N. Zhao and H.-J. Zhang, *Chemical Communications*, 2014, **50**, 6406.
54. J. Wang, J. Zhang, F. Jin, Y. Luo, S. Wang, Z. Zhang, Y. Wu, H. Liu, J. Y. Luc and M. Fang, *Crystengcomm*, 2015, **17**, 5906.
55. Z. Zhang, H. T. H. Nguyen, S. A. Miller, A. M. Ploskonka, J. B. DeCoste and S. M. Cohen, *Journal of the American Chemical Society*, 2015, **138**, 920.
56. Y. Lin, Q. Zhang, C. Zhao, H. Li, C. Kong, C. Shen and L. Chen, *Chemical Communications*, 2015, **51**, 697.
57. S. Sanda, S. Biswas and S. Konar, *Inorganic Chemistry*, 2015, **54**, 1218.
58. J. R. Karra, H. Jasuja, Y.-G. Huang and K. S. Walton, *Journal of Materials Chemistry A*, 2015, **3**, 1624.
59. S. Begum, S. Horike, S. Kitagawa and H. Krautscheid, *Dalton Transactions*, 2015, **44**, 18727.
60. J. H. Wang, M. Li and D. Li, *Chemistry*, 2014, **20**, 12004.
61. E.-L. Zhou, C. Qin, P. Huang, X.-L. Wang, W.-C. Chen, K.-Z. Shao and Z.-M. Su, *Chemistry-a European Journal*, 2015, **21**, 11894.
62. S. Galli, A. Maspero, C. Giacobbe, G. Palmisano, L. Nardo, A. Comotti, I. Bassanetti, P. Sozzani and N. Masciocchi, *Journal of Materials Chemistry A*, 2014, **2**, 12208.
63. K. Wang, X.-L. Lv, D. Feng, J. Li, S. Chen, J. Sun, L. Song, Y. Xie, J.-R. Li and H.-C. Zhou, *Journal of the American Chemical Society*, 2016, **138**, 914.
64. X.-Z. Song, S.-Y. Song, S.-N. Zhao, Z.-M. Hao, M. Zhu, X. Meng, L.-L. Wu and H.-J. Zhang, *Advanced Functional Materials*, 2014, **24**, 4034.
65. B. Saccoccia, A. M. Bohnsack, N. W. Waggoner, K. H. Cho, J. S. Lee, D.-Y. Hong, V. M. Lynch, J.-S. Chang and S. M. Humphrey, *Angewandte Chemie-International Edition*, 2015, **54**, 5394.
66. D. Wang, L. Zhang, G. Li, Q. Huo and Y. Liu, *RSC Advances*, 2015, **5**, 18087.
67. J. M. Taylor, R. Vaidyanathan, S. S. Iremonger and G. K. Shimizu, *J Am Chem Soc*, 2012, **134**, 14338.
68. N. Nijem, P. Canepa, U. Kaipa, K. Tan, K. Roodenko, S. Tekarli, J. Halbert, I. W. Oswald, R. K. Arvapally, C. Yang, T. Thonhauser, M. A. Omary and Y. J. Chabal, *Journal of the American Chemical Society*, 2013, **135**, 12615.
69. C. Yang, U. Kaipa, Q. Z. Mather, X. Wang, V. Nesterov, A. F. Venero and M. A. Omary, *Journal of the American Chemical Society*, 2011, **133**, 18094.
70. J. G. Nguyen and S. M. Cohen, *Journal of the American Chemical Society*, 2010, **132**, 4560.
71. X.-W. Zhu, X.-P. Zhou and D. Li, *Chemical Communications*, 2016, DOI: 10.1039/C6CC02116F.
72. X. Liu, Y. Li, Y. Ban, Y. Peng, H. Jin, H. Bux, L. Xu, J. Caro and W. Yang, *Chemical Communications*, 2013, **49**, 9140.
73. N. A. Khan, Z. Hasan and S. H. Jhung, *Journal of Hazardous Materials*, 2013, **244-245**, 444.
74. X. Lin, J. Jia, X. Zhao, K. M. Thomas, A. J. Blake, G. S. Walker, N. R. Champness, P. Hubberstey and M. Schroder, *Angewandte Chemie International Edition*, 2006, **45**, 7358.
75. Y.-C. He, J. Yang, W.-Q. Kan, H.-M. Zhang, Y.-Y. Liu and J.-F. Ma, *Journal of Materials Chemistry A*, 2015, **3**, 1675.
76. L. Sun, M. G. Campbell and M. Dinca, *Angewandte Chemie International Edition*, 2016, **55**, 3566.
77. S. Tominaka, F. X. Coudert, T. D. Dao, T. Nagao and A. K. Cheetham, *Journal of the American Chemical Society*, 2015, **137**, 6428.
78. S. Horike, D. Umeyama and S. Kitagawa, *Accounts of Chemical Research*, 2013, **46**, 2376.
79. M. Yoon, K. Suh, S. Natarajan and K. Kim, *Angewandte Chemie International Edition*, 2013, **52**, 2688.
80. L. E. Kreno, K. Leong, O. K. Farha, M. Allendorff, R. P. Van Duyne and J. T. Hupp, *Chemical Reviews*, 2012, **112**, 1105.
81. M. Yoon, R. Srirambalaji and K. Kim, *Chemical Reviews*, 2012, **112**, 1196.
82. L. Alaerts, E. Séguin, H. Poelman, F. Thibault-Starzyk, P. A. Jacobs and D. E. De Vos, *Chemistry – A European Journal*, 2006, **12**, 7353.
83. F. G. Cirujano, F. X. Llabres i Xamena and A. Corma, *Dalton Transactions*, 2012, **41**, 4249.
84. Y. K. Hwang, D.-Y. Hong, J.-S. Chang, S. H. Jhung, Y.-K. Seo, J. Kim, A. Vimont, M. Daturi, C. Serre and G. Férey, *Angewandte Chemie International Edition*, 2008, **47**, 4144.
85. S. Qiu, M. Xue and G. Zhu, *Chemical Society Reviews*, 2014, **43**, 6116.
86. P. Z. Ray and H. J. Shipley, *RSC Advances*, 2015, **5**, 29885.
87. S. J. Tesh and T. B. Scott, *Advanced Materials*, 2014, **26**, 6056.
88. B. Van de Voorde, B. Bueken, J. Denayer and D. De Vos, *Chemical Society Reviews*, 2014, **43**, 5766.
89. P. Küsgens, M. Rose, I. Senkovska, H. Fröde, A. Henschel, S. Siegle and S. Kaskel, *Microporous and Mesoporous Materials*, 2009, **120**, 325.
90. H. Furukawa, F. Gandara, Y. B. Zhang, J. Jiang, W. L. Queen, M. R. Hudson and O. M. Yaghi, *Journal of the American Chemical Society*, 2014, **136**, 4369.

91. I. Ali, *Chemical Reviews*, 2012, **112**, 5073.
92. B.-J. Zhu, X.-Y. Yu, Y. Jia, F.-M. Peng, B. Sun, M.-Y. Zhang, T. Luo, J.-H. Liu and X.-J. Huang, *The Journal of Physical Chemistry C*, 2012, **116**, 8601.
93. T. Grant Glover, G. W. Peterson, B. J. Schindler, D. Britt and O. Yaghi, *Chemical Engineering Science*, 2011, **66**, 163.
94. C. Montoro, F. Linares, E. Q. Procopio, I. Senkowska, S. Kaskel, S. Galli, N. Masciocchi, E. Barea and J. A. Navarro, *Journal of the American Chemical Society*, 2011, **133**, 11888.
95. J. Duan, W. Jin and R. Krishna, *Inorganic Chemistry*, 2015, **54**, 4279.
96. O. V. Gutov, W. Bury, D. A. Gomez-Gualdrón, V. Krungleviciute, D. Fairen-Jimenez, J. E. Mondloch, A. A. Sarjeant, S. S. Al-Juaid, R. Q. Snurr, J. T. Hupp, T. Yildirim and O. K. Farha, *Chemistry*, 2014, **20**, 12389.
97. A. M. Fracaroli, H. Furukawa, M. Suzuki, M. Dodd, S. Okajima, F. Gándara, J. A. Reimer and O. M. Yaghi, *Journal of the American Chemical Society*, 2014, **136**, 8863.
98. T. M. McDonald, J. A. Mason, X. Kong, E. D. Bloch, D. Gygi, A. Dani, V. Crocella, F. Giordanino, S. O. Odoh, W. S. Drisdell, B. Vlasisavljević, A. L. Dzubak, R. Poloni, S. K. Schnell, N. Planas, K. Lee, T. Pascal, L. F. Wan, D. Prendergast, J. B. Neaton, B. Smit, J. B. Kortright, L. Gagliardi, S. Bordiga, J. A. Reimer and J. R. Long, *Nature*, 2015, **519**, 303.
99. P.-Q. Liao, H. Chen, D.-D. Zhou, S.-Y. Liu, C.-T. He, Z. Rui, H. Ji, J.-P. Zhang and X.-M. Chen, *Energy & Environmental Science*, 2015, **8**, 1011.
100. J. Chun, S. Kang, N. Park, E. J. Park, X. Jin, K.-D. Kim, H. O. Seo, S. M. Lee, H. J. Kim, W. H. Kwon, Y.-K. Park, J. M. Kim, Y. D. Kim and S. U. Son, *Journal of the American Chemical Society*, 2014, **136**, 6786.
101. H. Jin, Y. Li, X. Liu, Y. Ban, Y. Peng, W. Jiao and W. Yang, *Chemical Engineering Science*, 2015, **124**, 170.
102. L. Xie, D. Liu, H. Huang, Q. Yang and C. Zhong, *Chemical Engineering Journal*, 2014, **246**, 142.
103. K.-Y. Andrew Lin and W.-D. Lee, *Chemical Engineering Journal*, 2016, **284**, 1017.
104. T. Han, Y. Xiao, M. Tong, H. Huang, D. Liu, L. Wang and C. Zhong, *Chemical Engineering Journal*, 2015, **275**, 134.
105. F. Leng, W. Wang, X. J. Zhao, X. L. Hu and Y. F. Li, *Colloids and Surfaces A: Physicochemical and Engineering Aspects*, 2014, **441**, 164.
106. X. Zhu, B. Li, J. Yang, Y. Li, W. Zhao, J. Shi and J. Gu, *Acs Applied Materials & Interfaces*, 2015, **7**, 223.
107. Y. S. Seo, N. A. Khan and S. H. Jhung, *Chemical Engineering Journal*, 2015, **270**, 22.
108. N. A. Khan, B. K. Jung, Z. Hasan and S. H. Jhung, *Journal of Hazardous Materials*, 2015, **282**, 194.
109. M. Carboni, C. W. Abney, S. Liu and W. Lin, *Chemical Science*, 2013, **4**, 2396.
110. A. J. Howarth, M. J. Katz, T. C. Wang, A. E. Platero-Prats, K. W. Chapman, J. T. Hupp and O. K. Farha, *Journal of the American Chemical Society*, 2015, **137**, 7488.
111. A. J. Howarth, T. C. Wang, S. S. Al-Juaid, S. G. Aziz, J. T. Hupp and O. K. Farha, *Dalton Transactions*, 2015, **45**, 93.
112. C. Wang, X. Liu, J. P. Chen and K. Li, *Scientific Reports*, 2015, **5**, 16613.
113. N. Zhang, X. Yang, X. Yu, Y. Jia, J. Wang, L. Kong, Z. Jin, B. Sun, T. Luo and J. Liu, *Chemical Engineering Journal*, 2014, **252**, 220.
114. Z. Hasan and S. H. Jhung, *Journal of Hazardous Materials*, 2015, **283**, 329.
115. Q.-R. Fang, D.-Q. Yuan, J. Sculley, J.-R. Li, Z.-B. Han and H.-C. Zhou, *Inorganic Chemistry*, 2010, **49**, 11637.
116. X. Zhao, D. Liu, H. Huang, W. Zhang, Q. Yang and C. Zhong, *Microporous and Mesoporous Materials*, 2014, **185**, 72.
117. T. A. Vu, G. H. Le, C. D. Dao, L. Q. Dang, K. T. Nguyen, Q. K. Nguyen, P. T. Dang, H. T. K. Tran, Q. T. Duong, T. V. Nguyen and G. D. Lee, *RSC Advances*, 2015, **5**, 5261.
118. J. Li, Y.-n. Wu, Z. Li, B. Zhang, M. Zhu, X. Hu, Y. Zhang and F. Li, *The Journal of Physical Chemistry C*, 2014, **118**, 27382.
119. B. Seoane, J. Coronas, I. Gascon, M. E. Benavides, O. Karvan, J. Caro, F. Kapteijn and J. Gascon, *Chemical Society Reviews*, 2015, **44**, 2421.
120. N. Rangnekar, N. Mittal, B. Elyassi, J. Caro and M. Tsapatsis, *Chemical Society Reviews*, 2015, **44**, 7128.
121. H. Guo, G. Zhu, I. J. Hewitt and S. Qiu, *Journal of the American Chemical Society*, 2009, **131**, 1646.
122. Y.-S. Li, H. Bux, A. Feldhoff, G.-L. Li, W.-S. Yang and J. Caro, *Advanced Materials*, 2010, **22**, 3322.
123. Y. Peng, Y. Li, Y. Ban, H. Jin, W. Jiao, X. Liu and W. Yang, *Science*, 2014, **346**, 1356.
124. A. Huang, W. Dou and J. Caro, *Journal of the American Chemical Society*, 2010, **132**, 15562.
125. A. Huang and J. Caro, *Angewandte Chemie International Edition*, 2011, **50**, 4979.
126. X. Liu, H. Jin, Y. Li, H. Bux, Z. Hu, Y. Ban and W. Yang, *Journal of Membrane Science*, 2013, **428**, 498.
127. Y. Hu, X. Dong, J. Nan, W. Jin, X. Ren, N. Xu and Y. M. Lee, *Chemical Communications*, 2011, **47**, 737.
128. X. Liu, N. K. Demir, Z. Wu and K. Li, *Journal of the American Chemical Society*, 2015, **137**, 6999.
129. A. Sotito, G. Orcajo, J. Maria Arsuaga, G. Calleja and J. Landaburu-Aguirre, *Journal of Applied Polymer Science*, 2015, **132**.
130. A. Kasik, X. Dong and Y. S. Lin, *Microporous and Mesoporous Materials*, 2015, **204**, 99.
131. J. Yao and H. Wang, *Chemical Society Reviews*, 2014, **43**, 4470.
132. C.-H. Kang, Y.-F. Lin, Y.-S. Huang, K.-L. Tung, K.-S. Chang, J.-T. Chen, W.-S. Hung, K.-R. Lee and J.-Y. Lai, *Journal of Membrane Science*, 2013, **438**, 105.
133. Y. Liu, E. Hu, E. A. Khan and Z. Lai, *Journal of Membrane Science*, 2010, **353**, 36.
134. X. Dong and Y. S. Lin, *Chemical Communications*, 2013, **49**, 1196.
135. Y. Li, L. H. Wee, J. A. Martens and I. F. J. Vankelecom, *Journal of Materials Chemistry A*, 2014, **2**, 10034.
136. A. Huang, N. Wang, C. Kong and J. Caro, *Angewandte Chemie International Edition*, 2012, **51**, 10551.
137. A. Huang, Y. Chen, N. Wang, Z. Hu, J. Jiang and J. Caro, *Chemical Communications*, 2012, **48**, 10981.
138. L. Dumeé, L. He, M. Hill, B. Zhu, M. Duke, J. Schutz, F. She, H. Wang, S. Gray, P. Hodgson and L. Kong, *Journal of Materials Chemistry A*, 2013, **1**, 9208.
139. G. M. Shi, T. Yang and T. S. Chung, *Journal of Membrane Science*, 2012, **415–416**, 577.
140. X.-L. Liu, Y.-S. Li, G.-Q. Zhu, Y.-J. Ban, L.-Y. Xu and W.-S. Yang, *Angewandte Chemie International Edition*, 2011, **50**, 10636.
141. H. Zhang, D. Liu, Y. Yao, B. Zhang and Y. S. Lin, *Journal of Membrane Science*, 2015, **485**, 103.
142. Y. Li, F. Liang, H. Bux, W. Yang and J. Caro, *Journal of Membrane Science*, 2010, **354**, 48.
143. H. Jin, X. Liu, Y. Ban, Y. Peng, W. Jiao, P. Wang, A. Guo, Y. Li and W. Yang, *Chemical Engineering Journal*, 2015, DOI: 10.1016/j.cej.2015.10.115.
144. R. Zhang, S. Ji, N. Wang, L. Wang, G. Zhang and J.-R. Li, *Angewandte Chemie International Edition*, 2014, **53**, 9775.
145. H. B. T. Jeazet, C. Staudt and C. Janiak, *Chemical Communications*, 2012, **48**, 2140.
146. M. S. Denny, Jr. and S. M. Cohen, *Angewandte Chemie International Edition*, 2015, **54**, 9029.
147. Z. Hu, B. J. Deibert and J. Li, *Chemical Society Reviews*, 2014, **43**, 5815.
148. Y. Zhang, Y. Chen, Y. Zhang, H. Cong, B. Fu, S. Wen and S. Ruan, *Journal of Nanoparticle Research*, 2013, **15**.
149. S.-I. Ohira, Y. Miki, T. Matsuzaki, N. Nakamura, Y.-k. Sato, Y. Hirose and K. Toda, *Analytica Chimica Acta*, 2015, **886**, 188.
150. L. Li, X. Jiao, D. Chen, B. V. Lotsch and C. Li, *Chemistry of Materials*, 2015, **27**, 7601.
151. Y. Yu, X.-M. Zhang, J.-P. Ma, Q.-K. Liu, P. Wang and Y.-B. Dong, *Chemical Communications*, 2014, **50**, 1444.
152. A. Douvali, A. C. Tsiplis, S. V. Eliseeva, S. Petoud, G. S. Papaefstathiou, C. D. Malliakas, I. Papadas, G. S. Armatas, I.

- Margiolaki, M. G. Kanatzidis, T. Lazarides and M. J. Manos, *Angewandte Chemie-International Edition*, 2015, **54**, 1651.
153. B. J. Deibert and J. Li, *Chemical Communications*, 2014, **50**, 9636.
154. J. Aguilera-Sigalat and D. Bradshaw, *Chemical Communications*, 2014, **50**, 4711.
155. P. Wu, Y. Liu, Y. Liu, J. Wang, Y. Li, W. Liu and J. Wang, *Inorganic Chemistry*, 2015, **54**, 11046.
156. C. Shao and Z.-M. Su, *Inorganic Chemistry Communications*, 2015, **57**, 4.
157. J.-N. Hao and B. Yan, *Chemical Communications*, 2015, **51**, 7737.
158. C. Liu and B. Yan, *Journal of Colloid and Interface Science*, 2015, **459**, 206.
159. Y. Zhou, H.-H. Chen and B. Yan, *Journal of Materials Chemistry A*, 2014, **2**, 13691.
160. X.-Y. Xu and B. Yan, *Acs Applied Materials & Interfaces*, 2015, **7**, 721.
161. B. Joarder, A. V. Desai, P. Samanta, S. Mukherjee and S. K. Ghosh, *Chemistry-a European Journal*, 2015, **21**, 965.
162. S. S. Nagarkar, A. V. Desai, P. Samanta and S. K. Ghosh, *Dalton Transactions*, 2015, **44**, 15175.
163. V. Pentyala, P. Davydovskaya, M. Ade, R. Pohle and G. Urban, *Sensors and Actuators B-Chemical*, 2016, **222**, 904.
164. Y.-X. Shi, F.-L. Hu, W.-H. Zhang and J.-P. Lang, *Crystengcomm*, 2015, **17**, 9404.
165. E. Zhou, Y. Zhang, Y. Li and X. He, *Electroanalysis*, 2014, **26**, 2526.
166. J. Cui, Y.-L. Wong, M. Zeller, A. D. Hunter and Z. Xu, *Angewandte Chemie-International Edition*, 2014, **53**, 14438.
167. A. Weiss, N. Reimer, N. Stock, M. Tiemann and T. Wagner, *Microporous and Mesoporous Materials*, 2016, **220**, 39.
168. A. Weiss, N. Reimer, N. Stock, M. Tiemann and T. Wagner, *Physical Chemistry Chemical Physics*, 2015, **17**, 21634.
169. S. Dong, G. Suo, N. Li, Z. Chen, L. Peng, Y. Fu, Q. Yang and T. Huang, *Sensors and Actuators B-Chemical*, 2016, **222**, 972.
170. J.-J. Liu, Y.-F. Guan, M.-J. Lin, C.-C. Huang and W.-X. Dai, *Crystal Growth & Design*, 2015, **15**, 5040.
171. P. Kumar, A. K. Paul and A. Deep, *Microporous and Mesoporous Materials*, 2014, **195**, 60.
172. L. Ma, C. Abney and W. Lin, *Chemical Society Reviews*, 2009, **38**, 1248.
173. J.-S. Qin, D.-Y. Du, W. Guan, X.-J. Bo, Y.-F. Li, L.-P. Guo, Z.-M. Su, Y.-Y. Wang, Y.-Q. Lan and H.-C. Zhou, *Journal of the American Chemical Society*, 2015, **137**, 7169.
174. N. Kornienko, Y. Zhao, C. S. Kley, C. Zhu, D. Kim, S. Lin, C. J. Chang, O. M. Yaghi and P. Yang, *Journal of the American Chemical Society*, 2015, **137**, 14129.
175. J. Bonnefoy, A. Legrand, E. A. Quadrelli, J. Canivet and D. Farrusseng, *Journal of the American Chemical Society*, 2015, **137**, 9409.
176. H. Fei, J. Shin, Y. S. Meng, M. Adelhardt, J. Sutter, K. Meyer and S. M. Cohen, *Journal of the American Chemical Society*, 2014, **136**, 4965.
177. W. Zhang, G. Lu, C. Cui, Y. Liu, S. Li, W. Yan, C. Xing, Y. R. Chi, Y. Yang and F. Huo, *Advanced Materials*, 2014, **26**, 4056.
178. J. E. Mondloch, M. J. Katz, W. C. Isley Iii, P. Ghosh, P. Liao, W. Bury, G. W. Wagner, M. G. Hall, J. B. DeCoste, G. W. Peterson, R. Q. Snurr, C. J. Cramer, J. T. Hupp and O. K. Farha, *Nature Materials*, 2015, **14**, 512.
179. J. Jiang, F. Gándara, Y.-B. Zhang, K. Na, O. M. Yaghi and W. G. Klemperer, *Journal of the American Chemical Society*, 2014, **136**, 12844.
180. H. Wan, C. Chen, Z. Wu, Y. Que, Y. Feng, W. Wang, L. Wang, G. Guan and X. Liu, *ChemCatChem*, 2015, **7**, 441.
181. Y. Zang, J. Shi, X. Zhao, L. Kong, F. Zhang and Y. Zhong, *Reaction Kinetics, Mechanisms and Catalysis*, 2013, **109**, 77.
182. M. G. Goesten, J. Juan-Alcañiz, E. V. Ramos-Fernandez, K. B. Sai Sankar Gupta, E. Stavitski, H. van Bekkum, J. Gascon and F. Kapteijn, *Journal of Catalysis*, 2011, **281**, 177.
183. A. Herbst, A. Khutia and C. Janiak, *Inorganic Chemistry*, 2014, **53**, 7319.
184. D.-D. Liang, S.-X. Liu, F.-J. Ma, F. Wei and Y.-G. Chen, *Advanced Synthesis & Catalysis*, 2011, **353**, 733.
185. K. Meyer, M. Ranocchiaro and J. A. van Bokhoven, *Energy & Environmental Science*, 2015, **8**, 1923.
186. L. Valenzano, B. Civalieri, S. Chavan, S. Bordiga, M. H. Nilsson, S. Jakobsen, K. P. Lillerud and C. Lamberti, *Chemistry of Materials*, 2011, **23**, 1700.
187. Q. Liu, L. Ning, S. Zheng, M. Tao, Y. Shi and Y. He, *Scientific Reports*, 2013, **3**, 2916.
188. P. Serra-Crespo, E. V. Ramos-Fernandez, J. Gascon and F. Kapteijn, *Chemistry of Materials*, 2011, **23**, 2565.
189. J. Gascon, U. Aktay, M. D. Hernandez-Alonso, G. P. M. van Klink and F. Kapteijn, *Journal of Catalysis*, 2009, **261**, 75.
190. C. Serre, F. Millange, C. Thouvenot, M. Noguès, G. Marsolier, D. Louër and G. Férey, *Journal of the American Chemical Society*, 2002, **124**, 13519.
191. Y. Fu, D. Sun, Y. Chen, R. Huang, Z. Ding, X. Fu and Z. Li, *Angewandte Chemie International Edition*, 2012, **51**, 3364.
192. D. Feng, Z. Y. Gu, J. R. Li, H. L. Jiang, Z. Wei and H. C. Zhou, *Angewandte Chemie International Edition*, 2012, **51**, 10307.
193. A. M. Marti, M. Van and K. J. Balkus, *Journal of Porous Materials*, 2014, **21**, 889.
194. S. Wang, Y. Hou, S. Lin and X. Wang, *Nanoscale*, 2014, **6**, 9930.
195. S. Wang, W. Yao, J. Lin, Z. Ding and X. Wang, *Angewandte Chemie International Edition*, 2014, **53**, 1034.
196. A. Dhakshinamoorthy, A. M. Asiri and H. Garcia, *Chemical Communications*, 2014, **50**, 12800.
197. J. Jiang and O. M. Yaghi, *Chemical Reviews*, 2015, **115**, 6966.
198. Q. Tang, Y. Liu, S. Liu, D. He, J. Miao, X. Wang, G. Yang, Z. Shi and Z. Zheng, *Journal of the American Chemical Society*, 2014, **136**, 12444.
199. P. Ramaswamy, N. E. Wong and G. K. H. Shimizu, *Chemical Society Reviews*, 2014, **43**, 5913.
200. M. Bazaga-García, M. Papadaki, R. M. P. Colodrero, P. Olivera-Pastor, E. R. Losilla, B. Nieto-Ortega, M. Á. G. Aranda, D. Choquesillo-Lazarte, A. Cabeza and K. D. Demadis, *Chemistry of Materials*, 2015, **27**, 424.
201. P. Ramaswamy, N. E. Wong, B. S. Gelfand and G. K. H. Shimizu, *Journal of the American Chemical Society*, 2015, **137**, 7640.
202. W. J. Phang, W. R. Lee, K. Yoo, D. W. Ryu, B. Kim and C. S. Hong, *Angewandte Chemie International Edition*, 2014, **53**, 8383.
203. M. Bazaga-Garcia, R. M. Colodrero, M. Papadaki, P. Garczarek, J. Zon, P. Olivera-Pastor, E. R. Losilla, L. Leon-Reina, M. A. Aranda, D. Choquesillo-Lazarte, K. D. Demadis and A. Cabeza, *Journal of the American Chemical Society*, 2014, **136**, 5731.
204. P. Barbosa, N. C. Rosero-Navarro, F.-N. Shi and F. M. L. Figueiredo, *Electrochimica Acta*, 2015, **153**, 19.
205. M. Sadakiyo, T. Yamada, K. Honda, H. Matsui and H. Kitagawa, *Journal of the American Chemical Society*, 2014, **136**, 7701.
206. S. S. Nagarkar, S. M. Unni, A. Sharma, S. Kurungot and S. K. Ghosh, *Angewandte Chemie International Edition*, 2014, **53**, 2638.
207. D. D. Borges, S. Devautour-Vinot, H. Jobic, J. Ollivier, F. Nouar, R. Semino, T. Devic, C. Serre, F. Paesani and G. Maurin, *Angewandte Chemie International Edition*, 2016, **55**, 3919.
208. W. J. Phang, H. Jo, W. R. Lee, J. H. Song, K. Yoo, B. Kim and C. S. Hong, *Angewandte Chemie International Edition*, 2015, **54**, 5142.
209. J. M. Taylor, T. Komatsu, S. Dekura, K. Otsubo, M. Takata and H. Kitagawa, *Journal of the American Chemical Society*, 2015, **137**, 11498.
210. S. Begum, Z. Wang, A. Donnadio, F. Costantino, M. Casciola, R. Valiullin, C. Chmelik, M. Bertmer, J. Karger, J. Haase and H. Krautscheid, *Chemistry*, 2014, **20**, 8862.
211. X. Y. Dong, X. P. Hu, H. C. Yao, S. Q. Zang, H. W. Hou and T. C. Mak, *Inorganic Chemistry*, 2014, **53**, 12050.
212. M. Sadakiyo, H. Kasai, K. Kato, M. Takata and M. Yamauchi, *Journal of the American Chemical Society*, 2014, **136**, 1702.
213. M. Sadakiyo, T. Yamada and H. Kitagawa, *Journal of the American Chemical Society*, 2014, **136**, 13166.
214. R. Ameloot, M. Aubrey, B. M. Wiers, A. P. Gomora-Figueroa, S. N. Patel, N. P. Balsara and J. R. Long, *Chemistry*, 2013, **19**, 5533.

ARTICLE

Journal Name

215. A. Planchais, S. Devautour-Vinot, F. Salles, F. Ragon, T. Devic, C. Serre and G. Maurin, *The Journal of Physical Chemistry C*, 2014, **118**, 14441.